AD-A039 751 WATERVLIET ARSENAL N Y F/G 19/6

EFFECTS OF PRESSURE AND THERMAL LOADINGS ON A THIN PLATING INSI--ETC(U)

MAR 77 S PU, J J WU

UNCLASSIFIED WVT-TR-77020 NL

1 OF 1

ADA039 751

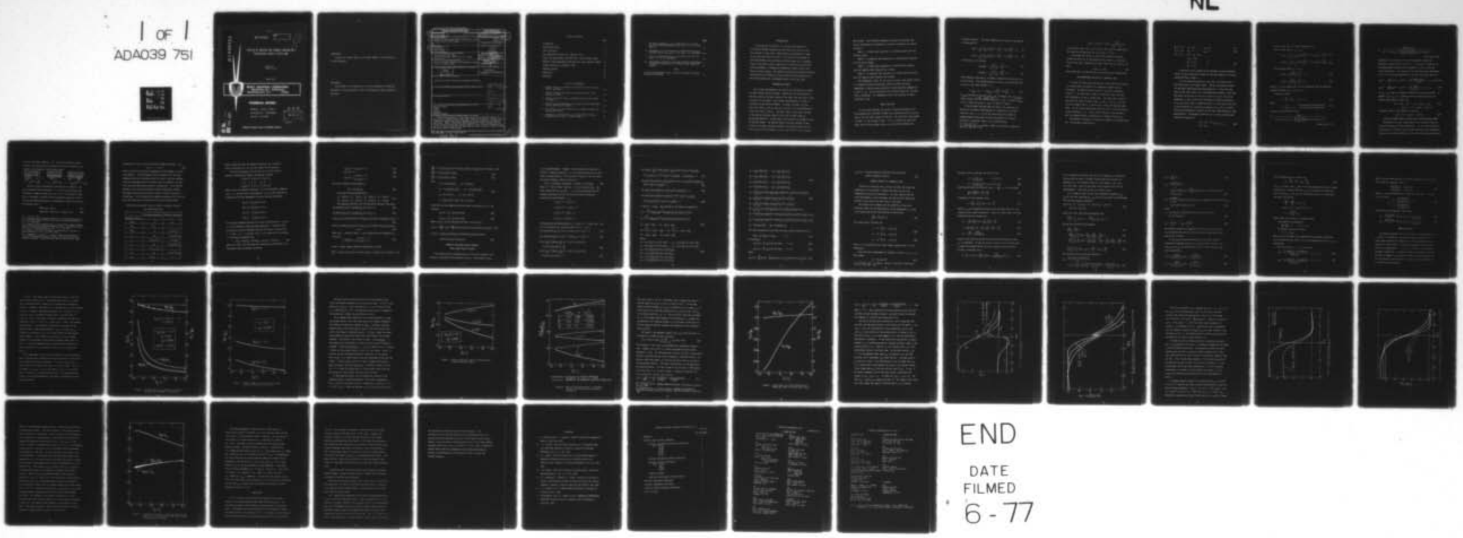

END

DATE FILMED

6-77

WVT-TR-77020

AD

EFFECTS OF PRESSURE AND THERMAL LOADINGS ON A THIN PLATING INSIDE A THICK TUBE

San-Li Pu
Julian J. Wu

March 1977

US ARMY
ARRADCOM
BENET WEAPONS LABORATORY
WATERVLIET ARSENAL
WATERVLIET, N.Y. 12189

TECHNICAL REPORT

AMCMS No. 611102.11.H4500

DA Project No. 1L161102AH45

Pron No. EJ-7-Y0011

DISPOSITION

Destroy this report when it is no longer needed. Do not return it to the originator.

DISCLAIMER

The findings in this report are not to be construed as an official Department of the Army position unless so designated by other authorized documents.

SECURITY CLASSIFICATION OF THIS PAGE (When Data Entered)

REPORT DOCUMENTATION PAGE

READ INSTRUCTIONS BEFORE COMPLETING FORM

1. REPORT NUMBER: (14) WVT-TR-77020	2. GOVT ACCESSION NO.
3. RECIPIENT'S CATALOG NUMBER: (9) Technical rept.	
4. TITLE (and Subtitle): (6) Effects of Pressure and Thermal Loadings on a Thin Plating Inside a Thick Tube.	5. TYPE OF REPORT & PERIOD COVERED
	6. PERFORMING ORG. REPORT NUMBER
7. AUTHOR(s): (10) San-Li Pu, Julian J. Wu	8. CONTRACT OR GRANT NUMBER(s)
9. PERFORMING ORGANIZATION NAME AND ADDRESS: Benet Weapons Laboratory, Watervliet Arsenal, Watervliet, N.Y. 12189, SARWV-RT-TP	10. PROGRAM ELEMENT, PROJECT, TASK AREA & WORK UNIT NUMBERS: (16) AMCMS No. 611102.11.H4500; DA Proj No. 1L161102AH45; Pron No. EJ-7-Y0011
11. CONTROLLING OFFICE NAME AND ADDRESS: US Army Armament Research and Development Command, Dover, New Jersey 07801	12. REPORT DATE: (11) March 1977
	13. NUMBER OF PAGES: 46
14. MONITORING AGENCY NAME & ADDRESS (if different from Controlling Office): (12) 45p.	15. SECURITY CLASS. (of this report): UNCLASSIFIED
	15a. DECLASSIFICATION/DOWNGRADING SCHEDULE

16. DISTRIBUTION STATEMENT (of this Report)

Approved for public release; distribution unlimited.

17. DISTRIBUTION STATEMENT (of the abstract entered in Block 20, if different from Report)

ACCESSION for
NTIS White Section
DDC Buff Section
UNANNOUNCED
JUSTIFICATION
BY
DISTRIBUTION/AVAILABILITY CODES
Dist. AVAIL. and/or SPECIAL
A

18. SUPPLEMENTARY NOTES

19. KEY WORDS (Continue on reverse side if necessary and identify by block number)

Composite Tubes
Cracks
Plating
Stresses
Thermal Stresses

20. ABSTRACT (Continue on reverse side if necessary and identify by block number)

Stress distribution in a thin layer of plating on the bore surface of a thick tube is studied based on the linear theory of elasticity. Several simple mathematical models are used to represent a variety of material and loading conditions. Results from these simple mathematical models indicate that the chrome plating in a gun tube is very likely to crack. Relative mechanical properties of plating materials and tube materials are discussed in order to reduce the stress level in the plating.

DD FORM 1 JAN 73 1473 EDITION OF 1 NOV 65 IS OBSOLETE

371 050

SECURITY CLASSIFICATION OF THIS PAGE (When Data Entered)

TABLE OF CONTENTS

LIST OF ILLUSTRATIONS

TABLE

INTRODUCTION

The purpose of this report is to present some analytical correlations between loadings and their mechanical effects on the thin plating in a gun tube. These effects are manifested in terms of the resulting stress and strain. The analytical techniques of continuum mechanics thus provide an efficient means for a systematic study of the plating stress condition for a variety of material and loading parameters. Although the mathematical models used in this report are quite simple, the extension extrapolated from this direction should prove to be valuable in the selection of plating materials or the plating process for a prolonged service life of gun tubes.

MATHEMATICAL MODELS

For a crude approximation, the tube may be considered as a hollow cylinder without the thin plating. Assume that the thin plating has the same strain as the bore surface of the tube, then the stress in the plating can be estimated. For a better approximation, the tube is considered as two hollow cylinders. The outer cylinder is of gun steel with radii r_c and r_2, the inner cylinder is of electrodeposited chrome with radii r_1 and r_c. The inner radius of the outer cylinder is the same as the outer radius of the inner cylinder under an unstressed condition. In both cases, the cylinders are assumed to have an infinite length. The applied loads on the bore surfaces of the cylinders are radial pressures uniformly distributed either over the entire length of the cylinders or over a semi-infinite axial range of

the cylinder. Four different mathematical models are obtained from various combinations of assumptions in material properties and loading conditions.

Model 1: A simple tube subjected to a uniform pressure over the infinite length.

Model 2: A composite tube subjected to a uniform radial pressure over the entire length.

Model 3: A simple tube subjected to a uniform radial pressure over the negative axial range of the cylinder.

Model 4: A composite tube subjected to a uniform radial pressure over the negative axial range of the cylinder.

The mathematical model for the study of steady state thermal effects is a composite tube with free ends; the bore surface maintains temperature T_1 and the outer cylindrical surface maintains temperature T_2 and $T_1 > T_2$. At the interface of two different materials, the heat flux is continuous. All temperature fields are functions of radial coordinate r only.

LAME'S SOLUTION

For very thin platings, the stress in the plating material can be estimated from a solution of model one, taking the strain to be the same as for the inner surface of the tube. The solution of the problem of model 1 is due to Lamé in 1852. Let r_1, r_2 denote the inner and outer radii of the cylinder, and p_1, p_2 the uniform internal and

external pressures. The stress components are given by, see page 59 of reference [1],

$$\sigma_r(r) = \frac{-1}{r_2^2 - r_1^2}\{p_2 r_2^2(1 - \frac{r_1^2}{r^2}) + p_1 r_1^2(\frac{r_2^2}{r^2} - 1)\} \quad (1)$$

$$\sigma_\theta(r) = \frac{-1}{r_2^2 - r_1^2}\{p_2 r_2^2(1 + \frac{r_1^2}{r^2}) - p_1 r_1^2(\frac{r_2^2}{r^2} + 1)\} \quad (2)$$

In the case $p_2 = 0$, we have

$$\sigma_r(r)/p_1 = -\frac{r_1^2}{r_2^2 - r_1^2}(\frac{r_2^2}{r^2} - 1) \quad (3)$$

$$\sigma_\theta(r)/p_1 = \frac{r_1^2}{r_2^2 - r_1^2}(\frac{r_2^2}{r^2} + 1) \quad (4)$$

These equations show that σ_r is always a compressive stress and σ_θ a tensile stress. The maximum compressive stress σ_r and tensile stress σ_θ occur at the inner surface $r = r_1$

$$|\sigma_r|_{max} = p_1 \quad , \quad (\sigma_\theta)_{max} = p_1(\frac{r_2^2}{r_1^2} + 1)/(\frac{r_2^2}{r_1^2} - 1) \quad (5)$$

$(\sigma_\theta)_{max}$ decreases as the wall ratio r_2/r_1 increases, and $(\sigma_\theta)_{max}$ is always greater than the internal pressure p_1. Let σ_{θ_o} denote $(\sigma_\theta)_{max}$ in (5), a graph of σ_{θ_o}/p_1 vs r_2/r_1 is shown in Figure 1.

If the cylinder has open ends and there is no constraint to prevent the cylinders from extension or contraction in the axial direction, then $\sigma_z = 0$. If, on the other hand, the cylinder is clamped between fixed planes so that displacement in the axial direction is prevented, then σ_z can be obtained from

[1] S. Timoshenko and J. N. Goodier, THEORY OF ELASTICITY, McGraw-Hill Book Co., New York, 1951.

$$\sigma_z(r) = \nu(\sigma_r(r) + \sigma_\theta(r)) = \frac{2\nu r_1^2}{(r_2^2 - r_1^2)} p_1$$

This equation shows that σ_z is a tensile stress and its magnitude is less than the minimum value of $\sigma_\theta(r)$ (since $\nu \leq 0.5$).

To estimate the stress $\sigma_{\theta 1}$ in the thin plating, we simply equate the strain $\varepsilon_{\theta 1}$ in the plating to the strain ε_θ at the bore of the thick tube. Neglecting the small effect due to σ_r and σ_z, we have

$$\sigma_{\theta 1}/E_1 = \sigma_{\theta o}/E_2 \tag{6}$$

where subscripts 1,2 indicate the plating and the tube respectively.

ONE-DIMENSIONAL SOLUTION OF A COMPOSITE TUBE

In order to assess more precisely the stress and strain condition in a plated tube, the problem of a composite cylinder must be considered. A composite tube consists of two tubes of different material. The inner tube is made of chrome with inner and outer radii denoted by r_1 and r_c respectively. The outer tube is made of gun steel with inner and outer radii r_c and r_2. Let E_1, E_2 be the elasticity modula and ν_1, ν_2 be Poisson's ratios of inner and outer tubes. At the initial unstressed condition, there is no force acting on the interface $r = r_c$. Let p_c be the pressure at the interface when the composite tube is submitted to an internal pressure p_1.

The problem is actually a rotationally symmetric, two-dimensional one. The boundary conditions are

$$\text{At } r = r_1: \quad \sigma_{r1} = -p_i \quad , \quad \tau_{rz1} = 0 \tag{7}$$

$$\text{At } r = r_2: \quad \sigma_{r2} = 0 \quad , \quad \tau_{rz2} = 0 \tag{8}$$

$$\text{At } r = r_c: \quad \left.\begin{aligned} \sigma_{r1} &= \sigma_{r2} = -p_c \\ \tau_{rz1} &= \tau_{rz2} \\ u_{r1} &= u_{r2} \\ u_{z1} &= u_{z2} \end{aligned}\right\} \tag{9}$$

A solution of this problem can be obtained by using the method similar to that described in detail for the odd symmetric (in z-axis) problem defined in model 4.

In a case where the plating is very thin, its effect on the bulk steel tube is, of course, small. The one-dimensional solution for the steel tube should hold reasonably well. As for the inner tube, we may first treat it as a one-dimensional problem. Then from the static equilibrium in the axial direction, we can find stress components τ_{rz} and σ_z due to the difference in material properties. If τ_{rz} and σ_z are small in comparison with σ_θ in the inner tube, that is, the correction on σ_θ due to the presence of τ_{rz} and σ_z is small, then the one-dimensional solution for the inner tube should be a good approximation. The boundary conditions (9) in the one-dimensional problem are replaced by

$$\left.\begin{aligned} \sigma_{r1} &= \sigma_{r2} = -p_c \\ u_{r1} &= u_{r2} \end{aligned}\right\} \text{ for } r = r_c \tag{10}$$

Using (1) and (2), the stress components are:

For the inner tube, $r_1 \leq r \leq r_c$,

$$\sigma_{r1}(r) = \frac{-1}{r_c^2 - r_1^2}\{p_1 r_1^2(\frac{r_c^2}{r^2} - 1) + p_c r_c^2(1 - \frac{r_1^2}{r^2})\} \quad (11)$$

$$\sigma_{\theta 1}(r) = \frac{-1}{r_c^2 - r_1^2}\{p_1 r_1^2(\frac{r_c^2}{r^2} + 1) - p_c r_c^2(1 + \frac{r_1^2}{r^2})\} \quad (12)$$

For the outer tube, $r_c \leq r \leq r_2$,

$$\sigma_{r2}(r) = \frac{-\ p_c r_c^2}{r_2^2 - r_c^2}(\frac{r_2^2}{r^2} - 1) \quad (13)$$

$$\sigma_{\theta 2}(r) = \frac{p_c r_c^2}{r_2^2 - r_c^2}(\frac{r_2^2}{r^2} + 1) \quad (14)$$

Where p_c is still unknown and is to be determined from the remaining boundary condition $U_{r1} = U_{r2}$ at $r = r_c$.

From the relation

$$\varepsilon_\theta = \frac{U_r}{r} = \frac{1}{E}[\sigma_\theta - \nu(\sigma_r + \sigma_z) \quad (15)$$

Where

$$\sigma_z = \begin{cases} 0 & \text{for the state of plane stress} \\ \nu(\sigma_r + \sigma_\theta) & \text{for the state of plane strain} \end{cases} \quad (16)$$

We obtain two expressions for p_c

$$p_c = \frac{2p_1 r_1^2}{r_1^2 + r_c^2 - \nu_1(r_c^2 - r_1^2) + \frac{E_1}{E_2}\frac{(r_c^2 - r_1^2)}{(r_2^2 - r_c^2)}[r_2^2 + r_c^2 - \nu_2(r_2^2 - r_c^2)]},$$

plane stress (17)

$$p_c = \frac{2p_1 r_1^2(1-\nu_1)}{r_1^2 + (1-2\nu_1)r_c^2 + \frac{E_1}{E_2}\frac{(r_c^2-r_1^2)(1+\nu_2)}{(r_2^2-r_c^2)(1+\nu_1)}[r_2^2+(1-2\nu_2)r_c^2]} ,$$

plane strain (18)

Equations (17) or (18) and (11) to (14) determine radial and tangential stresses for any value of r. In the axial direction, we can approximately compute stress components σ_z and τ_{rz} from the static equilibrium. For instance, if we use plane stress formulation $\sigma_z(r) = 0$, the strain components for the inner and outer tubes are

$$\varepsilon_{z1}(r) = -\frac{\nu_1}{E_1}[\sigma_{r1}(r) + \sigma_{\theta 1}(r)] = -\frac{\nu_1}{E_1}\frac{2(p_1 r_1^2 - p_c r_c^2)}{r_c^2 - r_1^2} , \quad r_1 \le r \le r_c \tag{19}$$

$$\varepsilon_{z2}(r) = -\frac{\nu_2}{E_2}[\sigma_{r2}(r) + \sigma_{\theta 2}(r)] = -\frac{\nu_2}{E_2}\frac{2p_c r_c^2}{r_2^2 - r_c^2} , \quad r_c \le r \le r_2 \tag{20}$$

If $\varepsilon_{z1} = \varepsilon_{z2}$, then all boundary conditions in (9) are satisfied. In general, $\varepsilon_{z1} \neq \varepsilon_{z2}$, if ε_z denotes the final contraction per unit length of the composite tube, then

$$\sigma_{z1} = E_1(\varepsilon_z - \varepsilon_{z1}) \quad , \quad \sigma_{z2} = E_2(\varepsilon_z - \varepsilon_{z2}) \tag{21}$$
$$\sigma_{z1}(r_c^2 - r_1^2) + \sigma_{z2}(r_2^2 - r_c^2) = 0$$

The shear stress at the interface is given by

$$\tau_{rz}(r = r_c) = \sigma_{z1}(r_c^2 - r_1^2)/2r_c \tag{22}$$

SIMPLE TUBE UNDER RADIAL PRESSURE OVER A SEMI-INFINITE LENGTH

The objective of this investigation is to study the effect on stress distribution of load discontinuity. It is a basic problem in the study of an infinitely long cylinder subjected to an axisymmetric pressure distributed uniformly or arbitrarily on curved surfaces over

a part of the axial length [2 - 5]. From the principle of superposition, the problem may be considered as the sum of problem I and problem II illustrated in the following graph:

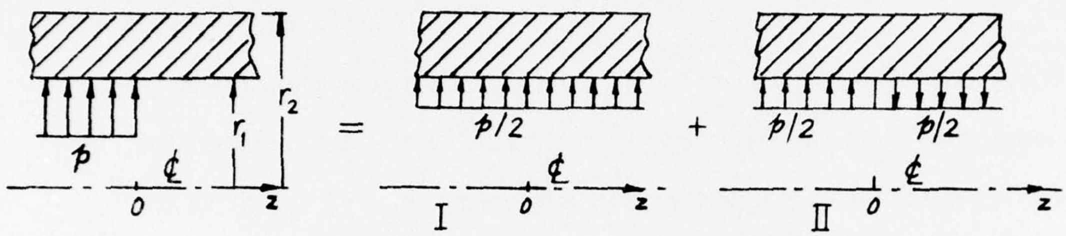

We have already discussed the Lamé solution of problem I. We shall concentrate here on problem II. In the case of torsion-free, rotationally symmetric about the z-axis, and in the absence of body forces, the general solution of the displacement equations of equilibrium, following Bonssinesq, is representable as the sum of the two displacement fields

$$2G[u,v,w] = \text{grad } \phi \tag{23}$$

$$2G[u,v,w] = \text{grad } (z\psi) - [0,0,4(1-\nu)\psi] \tag{24}$$

---

[2] C. J. Tranter, "On the Elastic Distortion of a Cylindrical Hole by a Localized Hydrostatic Pressure", Quarterly of Applied Mathematics, No. 4, p. 298, 1946.

[3] O. L. Bowie, "Elastic Stresses Due to a Semi-Infinite Band of Hydrostatic Pressure Acting Over a Cylindrical Hole in an Infinite Solid", Quarterly of Applied Mathematics, No. 5, p. 100, 1947.

[4] A. W. Rankin, "Shrink-Fit Stresses and Deformations", Journal of Applied Mechanics, Vol. 11, p. A77, 1944.

[5] P. P. Radkowski, J. Bluhm, O. L. Bowie, "Stresses and Strains in Elastic, Thick-Walled, Circular Cylinders Resulting from Axially Symmetric Loadings", Technical Report WAL No. 893/172, Dec. 1954.

provided $\phi(r,z)$ and $\psi(r,z)$ are arbitrary harmonic functions, i.e.,

$$\nabla^2\phi = 0 \quad , \quad \nabla^2\psi = 0 \tag{25}$$

Here [u,v,w] are the Cartesian components of displacement, G is the shear modulus. The displacement fields, equations (23) and (24), together with their associated fields of stress, which are obtained from the displacement-stress relations, will be referred to as the first and third Bonssinesq solutions, respectively. For a specific problem, a new solution obtained by certain combination of basic Bonssinesq solutions may be used in place of a basic solution for convenience. For our rotationally symmetric problem, we will use the first and fifth basic solutions defined by the following table:

STRESS AND DISPLACEMENT FIELDS IN TERMS OF HARMONIC FUNCTIONS AND THEIR DERIVATIVES

	1st Basic Solution	5th Basic Solution
Harmonic Function	ϕ	η
$2Gu_r$	ϕ_r	$r\eta_z$
$2Gu$	$r^{-1}\phi_\theta$	0
$2Gu_z$	ϕ_z	$-r\eta_r-4(1-\nu)\eta$
σ_r	ϕ_{rr}	$r\eta_{rz}+(1-2\nu)\eta_z$
σ	$r^{-1}\phi_r+r^{-2}\phi_\theta$	$(1-2\nu)\eta_z$
σ_z	ϕ_{zz}	$-r\eta_{rz}-2(2-\nu)\eta_z$
τ_r	$r^{-1}\phi_r - r^{-2}\phi_\theta$	0
τ_{rz}	ϕ_{rz}	$r\eta_{zz}-2(1-\nu)\eta_r$
$\tau_{\theta z}$	$r^{-1}\phi_{\theta z}$	0

Where a subscript after the harmonic function ϕ (or η) means a partial derivative of ϕ (or η) with respect to the subscript.

The stress functions, $\phi(r,\theta,z)$ and $\eta(r,\theta,z)$, must satisfy Laplace's equation which admits the product solutions

$$\begin{bmatrix} I_n(kr) \\ \text{or} \\ K_n(kr) \end{bmatrix} \begin{bmatrix} \text{Cos } n\theta \\ \text{or} \\ \text{Sin } n\theta \end{bmatrix} \begin{bmatrix} \text{Cos } kz \\ \text{or} \\ \text{Sin } kz \end{bmatrix}$$

where k and n are separate constants. For the rotationally symmetric case n = 0, and the load is odd symmetric in z, we shall confine our attention to the four aggregates of stress functions defined by

$$\phi_1(r,z) = \frac{1}{k^2} I_o(kr) \sin kz$$

$$\phi_2(r,z) = \frac{1}{k^2} K_o(kr) \sin kz$$

$$\eta_1(r,z) = -\frac{1}{k} I_o(kr) \cos kz$$

$$\eta_2(r,z) = -\frac{1}{k} K_o(kr) \cos kz$$

The solutions obtained from the first basic solution with $\phi = \phi_1$ and $\phi = \phi_2$ are denoted by $[S_A]$ and $[S_B]$ respectively. Similarly, $[S_C]$ and $[S_D]$ are solutions obtained from the fifth basic solution with $\eta = \eta_1$ and $\eta = \eta_2$. A solution, $[S]_k$, of the problem for an arbitrary k is obtained by superposition.

$$[S]_k = A(k)[S_A] + B(k)[S_B] + C(k)[S_C] + D(k)[S_D] \qquad (26)$$

Where A(k), B(k), C(k) and D(k) are superposition coefficients to be determined from the boundary conditions:

$$\tau_{rz}(r_1,z) = \tau_{rz}(r_2,z) = 0 \tag{27}$$

$$\sigma_r(r_2,z) = 0 \tag{28}$$

$$\sigma_r(r_1,z) = \begin{cases} p/2 \text{ for } z > 0 \\ -p/2 \text{ for } z < 0 \end{cases} \tag{29}$$

The final solution of the problem is

$$[S] = \int_o^\infty [S]_k \, dk \tag{30}$$

Using the following abbreviations

$$\begin{aligned} I_o &= I_o(kr_1), \quad I_1 = I_1(kr_1), \quad K_o = K_o(kr_1), \quad K_1 = K_1(kr_1) \\ \bar{I}_o &= I_o(kr_2), \quad \bar{I}_1 = I_1(kr_2), \quad \bar{K}_o = K_o(kr_2), \quad \bar{K}_1 = K_1(kr_2) \end{aligned} \tag{31}$$

The boundary conditions (27) to (29) may be written in the form:

$$AI_1-BK_1+C[kr_1I_o+2(1-\nu)I_1]+D[kr_1K_o-2(1-\nu)K_1] = 0 \tag{32}$$

$$A\bar{I}_1-B\bar{K}_1+C[kr_2\bar{I}_o+2(1-\nu)\bar{I}_1]+D[kr_2\bar{K}_o-2(1-\nu)\bar{K}_1] = 0 \tag{33}$$

$$A(kr_2\bar{I}_o-\bar{I}_1)+B(kr_2\bar{K}_o+\bar{K}_1)+C[(1-2\nu)kr_2\bar{I}_o+k^2r_2{}^2\bar{I}_1]+D[(1-2\nu)kr_2\bar{K}_o-k^2r_2{}^2\bar{K}_1] = 0 \tag{34}$$

$$A(kr_1I_o-I_1)+B(kr_1K_o+K_1)+C[(1-2\nu)kr_1I_o+k^2r_1{}^2I_1]+D[(1-2\nu)kr_1K_o-k^2r_1{}^2K_1] = pr_1/\pi \tag{35}$$

Where A,B,... are A(k), B(k),... and to obtain the last equation, we have used

$$\int_o^\infty \frac{\sin kz}{k} \, dk = \begin{cases} \pi/2 \text{ for } z > 0 \\ -\pi/2 \text{ for } z < 0 \end{cases} \tag{36}$$

After a rather lengthy algebraic manipulation, we have

$$\frac{A\pi\Delta}{pr_1} = (K_1-\bar{K}_1h_1{}')h_o{}'/h_1+2(1-\nu)(kr_1K_o-kr_2\bar{K}_oh_1{}')+\alpha_o[h_o\bar{K}_1-K_1-2(1-\nu)h_1\bar{K}_1] \tag{37}$$

$$\frac{B\pi\Delta}{pr_1} = (I_1-\bar{I}_1h_1')h_o'/h_1-2(1-\nu)(kr_1I_o-kr_2\bar{I}_oh_1')+\alpha_o[h_o\bar{I}_1-I_1-2(1-\nu)h_1\bar{I}_1] \quad (38)$$

$$\frac{C\pi\Delta}{pr_1} = -kr_1K_o+kr_2\bar{K}_oh_1'+\alpha_o\bar{K}_1h_1 \quad (39)$$

$$\frac{D\pi\Delta}{pr_1} = kr_1I_o-kr_2\bar{I}_oh_1'+\alpha_o\bar{I}_1h_1 \quad (40)$$

Here

$$h_o = kr_1(I_o\bar{K}_1+K_o\bar{I}_1) \quad , \quad h_1 = K_1\bar{I}_1-I_1\bar{K}_1$$

$$h_o' = kr_1kr_2(K_o\bar{I}_o-I_o\bar{K}_o) \quad , \quad h_1' = kr_2(I_1\bar{K}_o+K_1\bar{I}_o) \quad (41)$$

$$\alpha_o = 2(1-\nu)+k^2r_1^2 \quad , \quad \alpha_1 = 2(1-\nu)+k^2r_2^2$$

$$\Delta = \alpha_o(h_o^2-\alpha_1h_1^2)-(h_o'^2-\alpha_1h_1'^2)-(\alpha_o+\alpha_1)$$

Using (30), we can compute stress and strain at any point (r,z). For instance,

$$\sigma_\theta(r,z) = \int_o^\infty \sigma_\theta(r,k)\sin kz dk \quad (42)$$

$$\sigma_z(r,z) = \int_o^\infty \sigma_z(r,k)\sin kz dk \quad (43)$$

Where $\sigma_\theta(r,k)$ $\sigma_z(r,k)$ from (26) and Table 1 are given by

$$\sigma_\theta(r,k) = \frac{A(k)}{kr}I_1(kr)-\frac{B(k)}{kr}K_1(kr)+C(k)(1-2\nu)I_o(kr)+D(k)(1-2\nu)K_o(kr) \quad (44)$$

$$\sigma_z(r,k) = -A(k)I_o(kr)-B(k)K_o(kr)-C(k)[(4-2\nu)I_o(kr)+krI_1(kr)]$$
$$-D(k)[(4-2\nu)K_o(kr)-krK_1(kr)] \quad (45)$$

COMPOSITE TUBE UNDER RADIAL PRESSURE OVER A SEMI-INFINITE LENGTH

This problem may be considered again as the sum of problem I and problem II mentioned in the preceding section. Both problems I and

II are two-dimensional. However, the one-dimensional solution of problem I, obtained previously, is a good approximation for our thin layer of chrome plating. The solutions of problem II for the inner and outer cylinders, similar to (26), are

$$[S_i]_k = A_i(k)[S_A] + B_i(k)[S_B] + C_i(k)[S_C] + D_i(k)[S_D] \tag{46}$$

where i = 1 for the inner tube and i = 2 for the outer tube. The eight coefficients A_1, A_2, B_1, ..., are to be determined from the boundary conditions (27) to (29) and the following continuity conditions at the interface $r = r_c$.

$$\sigma_{r1}(r_c, z) = \sigma_{r2}(r_c, z)$$

$$\tau_{rz1}(r_c, z) = \tau_{rz2}(r_c, z)$$

$$U_{r1}(r_c, z) = U_{r2}(r_c, z)$$

$$U_{z1}(r_c, z) = U_{z2}(r_c, z)$$

Introducing the new abbreviations $\tilde{I}_o = I_o(kr_c)$, $\tilde{I}_1 = I_1(kr_c)$ etc., the set of 8 equations for the determination of $A_1,\ldots,D_2$ is

$$A_1 I_1 - B_1 K_1 + C_1[kr_1 I_o + 2(1-\nu_1) I_1] + D_1[kr_1 K_o - 2(1-\nu_1) K_1] = 0 \tag{47}$$

$$A_2 \bar{I}_1 - B_2 \bar{K}_1 + C_2[kr_2 \bar{I}_o + 2(1-\nu_2) \bar{I}_1] + D_2[kr_2 K_o - 2(1-\nu_2) \bar{K}_1] = 0 \tag{48}$$

$$A_1(I_o - \frac{1}{kr_1} I_1) + B_1(K_o + \frac{1}{kr_1} K_1) + C_1[(1-2\nu_1) I_o + kr_1 I_1]$$
$$+ D_1[(1-2\nu_1) K_o - kr_1 K_1] = \frac{p}{\pi k} \tag{49}$$

$$A_2(\bar{I}_o - \frac{1}{kr_2} \bar{I}) + B_2(\bar{K}_o + \frac{1}{kr_2} \bar{K}_1) + C_2[(1-2\nu_2) \bar{I}_o + kr_2 \bar{I}_1]$$
$$+ D_2[(1-2\nu_2) \bar{K}_o - kr_2 \bar{K}_1] = 0 \tag{50}$$

$$(A_1-A_2)(\tilde{I}_o-\frac{1}{kr_c}\tilde{I}_1)+(B_1-B_2)(\tilde{K}_o+\frac{1}{kr_c}\tilde{K}_1)+[(1-2\nu_1)C_1-(1-2\nu_2)C_2]\tilde{I}_o$$

$$+(C_1-C_2)kr_c\tilde{I}_1+[(1-2\nu_1)D_1-(1-2\nu_2)D_2]\tilde{K}_o-(D_1-D_2)kr_c\tilde{K}_1=0 \tag{51}$$

$$(A_1-A_2)\tilde{I}_1-(B_1-B_2)\tilde{K}_1+(C_1-C_2)kr_c\tilde{I}_o+2[(1-\nu_1)C_1-(1-\nu_2)C_2]\tilde{I}_1+(D_1-D_2)kr_c\tilde{K}_o$$
$$-2[(1-\nu_1)D_1-(1-\nu_2)D_2]\tilde{K}_1=0 \tag{52}$$

$$(A_1-\mu A_2)\tilde{I}_1-(B_1-\mu B_2)\tilde{K}_1+(C_1-\mu C_2)kr_c\tilde{I}_o+(D_1-\mu D_2)kr_c\tilde{K}_o=0 \tag{53}$$

$$(A_1-\mu A_2)\tilde{I}_o+(B_1-\mu B_2)\tilde{K}_o+(C_1-\mu C_2)kr_c\tilde{I}_1+4[(1-\nu_1)C_1-(1-\nu_2)C_2]\tilde{I}_o$$
$$-(D_1-\mu D_2)kr_c\tilde{K}_1+4[(1-\nu_1)D_1-(1-\nu_2)D_2]\tilde{K}_o=0 \tag{54}$$

in which $\mu = G_1/G_2$. The solution of the system of equations is

$$C_2=-\frac{pr_1}{\pi}(d_5d_8-d_6d_7)^{-1}[kr_cd_8(K_1\tilde{I}_o+I_1\tilde{K}_o)+d_6(I_1\tilde{K}_1-K_1\tilde{I}_1)]$$

$$D_2=\frac{pr_1}{\pi}(d_5d_8-d_6d_7)^{-1}[kr_cd_7(K_1\tilde{I}_o+I_1\tilde{K}_o)+d_5(I_1\tilde{K}_1-K_1\tilde{I}_1)]$$

$$C_1=d_1C_2+d_2D_2\quad,\quad D_1=d_3C_2+d_4D_2 \tag{55}$$

$$A_1=\frac{pr_1}{\pi}K_1-a_5C_1-a_3D_1\quad,\quad B_1=\frac{pr_1}{\pi}I_1+a_1C_1+a_7D_1$$

$$A_2=-a_6C_2-a_4D_2\quad,\quad B_2=a_2C_2+a_8D_2$$

where

$$a_1=k^2r_1^2(I_o^2-I_1^2)-2(1-\nu_1)I_1^2\quad,\quad a_2=k^2r_2^2(\bar{I}_o^2-\bar{I}_1^2)-2(1-\nu_2)\bar{I}_1^2$$
$$a_3=k^2r_1^2(K_o^2-K_1^2)-2(1-\nu_1)K_1^2\quad,\quad a_4=k^2r_2^2(\bar{K}_o^2-\bar{K}_1^2)-2(1-\nu_2)\bar{K}_1^2$$
$$a_5=k^2r_1^2(I_oK_o+I_1K_1)+2(1-\nu_1)(1+I_1K_1),$$
$$a_6=k^2r_2^2(\bar{I}_o\bar{K}_o+\bar{I}_1\bar{K}_1)+2(1-\nu_2)(1+\bar{I}_1\bar{K}_1) \tag{56}$$
$$a_7=k^2r_1^2(I_oK_o+I_1K_1)-2(1-\nu_1)(1-I_1K_1)$$
$$a_8=k^2r_2^2(\bar{I}_o\bar{K}_o+\bar{I}_1\bar{K}_1)-2(1-\nu_2)(1-\bar{I}_1\bar{K}_1)$$

$$b_1 = a_5\tilde{I}_o - a_1\tilde{K}_o - kr_c\tilde{I}_1 \quad , \quad b_2 = a_6\tilde{I}_o - a_2\tilde{K}_o - kr_c\tilde{I}_1$$

$$b_3 = a_3\tilde{I}_o - a_7\tilde{K}_o + kr_c\tilde{K}_1 \quad , \quad b_4 = a_4\tilde{I}_o - a_8\tilde{K}_o + kr_c\tilde{K}_1$$

$$b_5 = a_5\tilde{I}_1 + a_1\tilde{K}_1 - kr_c\tilde{I}_o \quad , \quad b_6 = a_6\tilde{I}_1 + a_2\tilde{K}_1 - kr_c\tilde{I}_o \tag{57}$$

$$b_7 = a_3\tilde{I}_1 + a_7\tilde{K}_1 - kr_c\tilde{K}_o \quad , \quad b_8 = a_4\tilde{I}_1 + a_8\tilde{K}_1 - kr_c\tilde{K}_o$$

$$d_1 = \frac{-1}{2(1-\nu_1)}\{(1-\mu)[kr_c(b_6\tilde{K}_o - b_2\tilde{K}_1) + b_6\tilde{K}_1] - 2(1-\nu_2)[1-2(1-\mu)kr_c\tilde{I}_o\tilde{K}_1]\}$$

$$d_2 = \frac{-1}{2(1-\nu_1)}(1-\mu)\{b_8\tilde{K}_1 + kr_c[b_8\tilde{K}_o - b_4\tilde{K}_1 + 4(1-\nu_2)\tilde{K}_o\tilde{K}_1]\} \tag{58}$$

$$d_3 = \frac{-1}{2(1-\nu_1)}(1-\mu)\{b_6\tilde{I}_1 - kr_c[b_6\tilde{I}_o + b_2\tilde{I}_1 - 4(1-\nu_2)\tilde{I}_o\tilde{I}_1]\}$$

$$d_4 = \frac{1}{2(1-\nu_1)}\{(1-\mu)[kr_c(b_8\tilde{I}_o + b_4\tilde{I}_1 - 4(1-\nu_2)\tilde{I}_1\tilde{K}_o) - b_8\tilde{I}_1] + 2(1-\nu_2)\}$$

$$d_5 = kr_c(b_2 - b_1d_1 - b_3d_3) + 2(1-\nu_1)(kr_c\tilde{K}_o - \tilde{K}_1)d_3 + 2(kr_c\tilde{I}_o + \tilde{I}_1)[(1-\nu_1)d_1 - (1-\nu_2)]$$

$$d_6 = kr_c(b_4 - b_1d_2 - b_3d_4) + 2(1-\nu_1)(kr_c\tilde{I}_o + \tilde{I}_1)d_2 + 2(kr_c\tilde{K}_o - \tilde{K}_1)[(1-\nu_1)d_4 - (1-\nu_2)]$$

$$d_7 = \mu b_6 - b_5d_1 - b_7d_3 \quad , \quad d_8 = \mu b_8 - b_5d_2 - b_1d_4$$

The final solutions for the inner and outer tubes of problem II are

$$[S_i] = \int_o^\infty [S_i]_k \sin kz dk \,, \qquad i = 1,2 \tag{59}$$

For instance,

$$\sigma_{\theta i}(r,z) = \int_o^\infty \sigma_{\theta i}(r,k) \sin kz dk \,, \qquad i = 1,2 \tag{60}$$

$$\sigma_{zi}(r,z) = \int_o^\infty \sigma_{zi}(r,k) \sin kz dk \,, \qquad i = 1,2 \tag{61}$$

Where

$$\sigma_{\theta i}(r,k) = \frac{A_i}{kr} I_1(kr) - \frac{B_i}{kr} K_1(kr) + C_i(1-2\nu_i)I_o(kr) + D_i(1-2\nu_i)K_o(kr) \tag{62}$$

$$\sigma_{zi}(r,k) = -A_i I_0(kr) - B_i K_0(kr) - C_i[(4-2\nu_i)I_0(kr) + krI_1(kr)]$$
$$-D_i[(4-2\nu_i)K_0(kr) - krK_1(kr)] \qquad (63)$$

THERMAL STRESSES IN A COMPOSITE TUBE

Consider an infinitely long, circular cylinder and assume the temperature in the cylinder is symmetrical about the axis and independent of the axial coordinate z. We shall suppose that the axial displacement is zero throughout and then we shall modify the solution to the case of the free ends [1, page 408].

On account of the symmetry and the uniformity in the axial direction, there will be three non-zero stress components σ_r, σ_θ and σ_z and these must satisfy the condition of equilibrium

$$\frac{d\sigma_r}{dr} + \frac{\sigma_r - \sigma_\theta}{r} = 0 \qquad (64)$$

The stress-strain relations are

$$\varepsilon_r - \alpha T = \frac{1}{E}[\sigma_r - \nu(\sigma_\theta + \sigma_z)]$$
$$\varepsilon_\theta - \alpha T = \frac{1}{E}[\sigma_\theta - \nu(\sigma_r + \sigma_z)] \qquad (65)$$

$$\varepsilon_z - \alpha T = \frac{1}{E}[\sigma_z - \nu(\sigma_r + \sigma_\theta)] \qquad (66)$$

where α is the coefficient of linear thermal expansion and T is the temperature.

Since the axial displacement is assumed to be zero, i.e., $\varepsilon_z = 0$, (66) becomes

$$\sigma_z = \nu(\sigma_r + \sigma_\theta) - \alpha ET \qquad (67)$$

[1]S. Timoshenko and J. N. Goodier, THEORY OF ELASTICITY, McGraw-Hill Book Co., New York, 1951.

Solving σ_r and σ_θ from (65) and (67) we find

$$\sigma_r = \frac{E}{(1+\nu)(1-2\nu)}\{(1-\nu)\varepsilon_r+\nu\varepsilon_\theta-(1+\nu)\alpha T\} \tag{68}$$

$$\sigma_\theta = \frac{E}{(1+\nu)(1-2\nu)}\{(1-\nu)\varepsilon_\theta+\nu\varepsilon_r-(1+\nu)\alpha T\} \tag{69}$$

Substituting these into (64) and using $\varepsilon_r = \frac{du}{dr}$, $\varepsilon_\theta = u/r$, we obtain

$$\frac{d}{dr}\left[\frac{1}{r}\frac{d(ru)}{dr}\right] = \frac{1+\nu}{1-\nu}\alpha\frac{dT}{dr} \tag{70}$$

Integration of this equation yields

$$u = \frac{1+\nu}{1-\nu}\alpha\frac{1}{r}\int_a^r Trdr + C_1 r + \frac{C_2}{r} \tag{71}$$

where C_1, C_2 are integration constants and the lower limit a in the integral can be chosen arbitrarily. Using (71), (68), (69), the final expressions for the stresses are

$$\sigma_r = -\frac{\alpha E}{1-\nu}\frac{1}{r^2}\int_a^r Trdr + \frac{E}{1+\nu}\left[\frac{C_1}{1-2\nu} - \frac{C_2}{r^2}\right] \tag{72}$$

$$\sigma_\theta = \frac{\alpha E}{1-\nu}\frac{1}{r^2}\int_a^r Trdr + \frac{E}{1+\nu}\left[\frac{C_1}{1-2\nu} + \frac{C_2}{r^2}\right] - \frac{\alpha ET}{1-\nu} \tag{73}$$

$$\sigma_z = -\frac{\alpha ET}{1-\nu} + \frac{2\nu EC_1}{(1-\nu)(1-2\nu)} \tag{74}$$

Equation (74) gives the normal force distribution required to keep $u_z = 0$ throughout. To get the thermal stresses in the cylinder which is free from external forces, we have to apply at the end of the cylinder a resultant force

$$R = \int_a^b -\sigma_z\, 2\pi rdr = \frac{2\pi\alpha E}{1-\nu}\int_a^b Trdr - \frac{2\nu EC_1}{(1+\nu)(1-2\nu)}\pi(b^2-a^2) \tag{75}$$

By Saint-Venant's principle, this force will produce at a sufficient distance from the ends a uniformly distributed stress $R/\pi(b^2-a^2)$, denoted by C_3. This uniform stress will not change σ_r and σ_θ but will add a term $-\nu C_3 r/E$ on the right side of equation (71) for the displacement u. The axial strain ε_z is given by C_3/E.

For a composite tube, we have four integration constants, C_{11}, C_{12} for the inner tube and C_{21}, C_{22} for the outer tube to be determined from the four boundary conditions.

$$\begin{gathered}\sigma_{r1}(r=r_1) = 0, \quad \sigma_{r2}(r=r_2) = 0, \quad \sigma_{r1}(r=r_c) = \sigma_{r2}(r=r_c), \\ u_1(r=r_c) = u_2(r=r_c)\end{gathered} \tag{76}$$

Using (71), (72), and (73) and observing that

$$\lim_{r\to r_1} \frac{1}{r} \int_{r_1}^{r} Trdr = 0 \quad , \quad \lim_{r\to r_1} \frac{1}{r^2} \int_{r_1}^{r} Trdr = 0$$

We have the following four equations

$$\frac{C_{11}}{1-2\nu_1} - \frac{C_{12}}{r_1^{\,2}} = 0 \tag{77}$$

$$-\frac{\alpha_2 E_2}{1-\nu_2}\frac{1}{r_c^{\,2}}\int_{r_c}^{r_2} Trdr + \frac{E_2}{1+\nu_2}\left[\frac{C_{21}}{1-2\nu_2} - \frac{C_{22}}{r_2^{\,2}}\right] = 0 \tag{78}$$

$$-\frac{\alpha_1 E_1}{1-\nu_1}\frac{1}{r_c^{\,2}}\int_{r_1}^{r_c} Trdr + \frac{E_1}{1+\nu_1}\left[\frac{C_{11}}{1-2\nu_1} - \frac{C_{12}}{r_c^{\,2}}\right] = \frac{E_2}{1+\nu_2}\left[\frac{C_{21}}{1-2\nu_2} - \frac{C_{22}}{r_2^{\,2}}\right] \tag{79}$$

$$\frac{1+\nu_1}{1-\nu_1}\frac{\alpha_1}{r_c}\int_{r_1}^{r_c} Trdr + C_{11}r_c + \frac{C_{12}}{r_c} = C_{21}r_c + \frac{C_{22}}{r_c} \tag{80}$$

The solution of this system of equations is

$$C_{11} = \frac{E_2(1+\nu_1)(1-2\nu_1)(r_2^{\,2}-r_c^{\,2})}{\Delta'}$$

$$\left\{\alpha_1 T_c\left[-\frac{1+\nu_1}{1-\nu_1} + \frac{E_1}{E_2}\frac{1+\nu_2}{1-\nu_1}\frac{r_2^{\,2}+(1-2\nu_2)r_c^{\,2}}{r_2^{\,2}-r_c^{\,2}}\right] + \frac{2\alpha_2(1+\nu_2)r_c^{\,2}}{r_2^{\,2}-r_c^{\,2}}T_{2c}\right\} \tag{81}$$

$$C_{12} = \frac{r_1^2}{1-2\nu_1} C_{11} \tag{82}$$

$$C_{21} = \frac{(1+\nu_2)(1-2\nu_2)}{\Delta'}$$

$$\{\alpha_1 E_1(1+\nu_1)2r_c^2 T_{c1} + \frac{\alpha_2 T_{2c}}{1-\nu_2}[E_1(1+\nu_2)(r_c^2-r_1^2)+E_2(1+\nu_1)(r_1^2+ (1-2\nu_1)r_c^2)]\} \tag{83}$$

$$C_{22} = \frac{(1+\nu_2)r_c^2}{(1-\nu_2)\ \Delta'}\{2\alpha_1 E_1(1+\nu_1)(1-\nu_2)r_2^2 T_{c1}+ \alpha_2 T_{2c}[E_2(1+\nu_1)(r_1^2+(1-2\nu_1)r_c^2) -E_1(1+\nu_2)(1-2\nu_2)(r_c^2-r_1^2)]\} \tag{84}$$

where

$$\Delta' = E_1(1+\nu_2)(r_c^2-r_1^2)[r_2^2+(1-2\nu_2)r_c^2]+E_2(1+\nu_1)(r_2^2-r_c^2) [r_1^2+(1-2\nu_1)r_c^2] \tag{85}$$

$$T_{c1} = \int_{r_1}^{r_c} Trdr \quad , \quad T_{2c} = \int_{r_c}^{r_2} Trdr \tag{86}$$

The thermal stresses in a composite tube for plane strain can be easily obtained from (72) to (74) provided the temperature distribution T(r) is known.

In the case of force free condition at the ends, the one-dimensional treatment can only give an approximate solution. We find C_{31} and C_{32}, the uniform axial stress in the inner and outer tubes respectively,

$$C_{31} = \frac{2\alpha_1 E_1}{(1-\nu_1)(r_c^2-r_1^2)} T_{c1} - \frac{2\nu_1 E_1 C_{11}}{(1+\nu_1)(1-2\nu_1)} \tag{87}$$

$$C_{32} = \frac{2\alpha_2 E_2}{(1-\nu_2)(r_2^2-r_c^2)} T_{2c} - \frac{2\nu_2 E_2 C_{21}}{(1+\nu_2)(1-2\nu_2)} \tag{88}$$

The corresponding axial strains are

$$\varepsilon_{z1} = \frac{C_{31}}{E_1} \quad \text{and} \quad \varepsilon_{z2} = \frac{C_{32}}{E_2} \tag{89}$$

If ε_{z2} is greater than ε_{z1} and if the bond between the tubes is strong, then there is a shearing stress τ_{rz} at the interface and additional axial stresses σ_{z1}' and σ_{z2}' are introduced which can be found from the static equilibrium.

$$\frac{\sigma_{z1}'}{E_1} - \frac{\sigma_{z2}'}{E_2} = \varepsilon_{z2} - \varepsilon_{z1}$$

$$\sigma_{z1}'(r_c^2-r_1^2) + \sigma_{z2}'(r_2^2-r_c^2) = 0$$

$$\tau_{rz} = \frac{r_c^2-r_1^2}{2r_c}\sigma_{z1}'$$

Steady state flow of heat in a composite tube:

The equation of conduction is

$$\frac{d}{dr}\left(r\frac{dT}{dr}\right) = 0 \qquad r_1 \leq r \leq r_2$$

The general solution of this is

$$T = A + B \log r$$

where A, B are constants to be determined from boundary conditions. For the composite tube, let T_1, T_c, T_2 be temperatures at $r=r_1$, r_c, r_2, respectively.

Then $T(r)$ where $r_1 < r < r_2$ is given by

$$T(r) = \frac{T_1 \log(r_c/r) + T_c \log(r/r_1)}{\log(r_c/r_1)} \qquad r_1 \leq r \leq r_c \tag{90}$$

$$T(r) = \frac{T_c \log(r_2/r) + T_2 \log(r/r_c)}{\log(r_2/r_c)} \qquad r_c \leq r \leq r_2 \tag{91}$$

where T_c can be found from the continuity condition of the flux over the surface of separation, that is

$$\frac{2\pi K_1(T_1-T_c)}{\log(r_c/r_1)} = \frac{2\pi K_2(T_c-T_2)}{\log(r_2/r_c)} \tag{92}$$

where K_1, K_2 are conductivities of inner and outer tubes. Solving for T_c, we have

$$T_c = \frac{T_1 + \dfrac{K_2}{K_1}\dfrac{\log(r_c/r_1)}{\log(r_2/r_c)} T_2}{1 + \dfrac{K_2}{K_1}\dfrac{\log(r_c/r_1)}{\log(r_2/r_c)}} \tag{93}$$

Using (90) or (91), equations (86) become

$$T_{c1} = \frac{T_c r_c^2 - T_1 r_1^2}{2} + \frac{1}{4}(T_1-T_c)(r_c^2-r_1^2)\frac{1}{\log(r_c/r_1)} \tag{94}$$

$$T_{2c} = \frac{T_2 r_2^2 - T_c r_c^2}{2} + \frac{1}{4}(T_c-T_2)(r_2^2-r_c^2)\frac{1}{\log(r_2/r_c)} \tag{95}$$

NUMERICAL RESULTS

The elastic constants of gun steel used in our computation are $\nu = 0.285$, $E = 30\text{x}10^6$ psi, and the yield point is $165\text{x}10^3$ psi. A large range of mechanical properties for electrodeposited chrome is reported in various books. The following average values are used in most of our computations: $\nu = 0.31$, $E = 20\text{x}10^6$ psi, the ultimate strength is $40\text{x}10^3$ psi. To study the effect of Poisson's ratio and the effect of modulus of elasticity on the stress distribution, we vary the value of ν from 0 to 0.5, the value of E from $15\text{x}10^6$ psi to $30\text{x}10^6$ psi for the chrome.

In Fig 1, the curve $\sigma_{\theta o}/p_1$ as a function of r_2/r_1 is for the Lamé solution, equation (5). The maximum hoop stress $\sigma_{\theta o}$ is often used to normalize other stresses in our presentation of numerical results. In model 1, the ratio of $\sigma_{\theta 1}$, the hoop stress in the plating, to $\sigma_{\theta o}$ is a constant, according to equation (6). For $E_2/E_1 = 1.5$, $\sigma_{\theta 1}/p_1$ vs r_2/r_1 is plotted in broken lines. The solid line of $\sigma_{\theta 1}/p_1$ vs r_2/r_1 is the results of model 2, equations (12) and (17), with $E_2/E_1 = 1.5$, $\nu_1 = 0.31$, $\nu_2 = 0.285$, $r_c/r_1 = 1.005$. The estimate based on model 1 is quite good in comparison to the model of the composite tube. After normalization by $\sigma_{\theta o}/p_1$, we have $\sigma_{\theta 1}/\sigma_{\theta o}$ plotted as a function of r_2/r_1 in the same figure for the composite tube of model 2. For a fixed r_2/r_1, the ratio $\sigma_{\theta 1}/\sigma_{\theta o}$ increases slightly if the thickness of the plating increases (see x and o in Fig 1). If we use equation (18), the plane strain formulation, in place of equation (17), the overall results will not change more than 2%.

Even though model 1 gives a good estimate on $\sigma_{\theta 1}$ in the plating, model 2 provides more information on stress variations in the plating due to changes of material properties. The ratio, E_2/E_1, has a large effect on the maximum hoop stress in the thin layer. In Fig 2, the graphs of $\sigma_{\theta 1}/\sigma_{\theta o}$ vs r_2/r_1 are shown for $E_2/E_1 = 1$, 1.5 and 2 with $\nu = 0.31$ and $\nu_2 = 0.285$ remaining fixed. The maximum tensile stress in the plating decreases as the modulus of elasticity of the plating decreases.

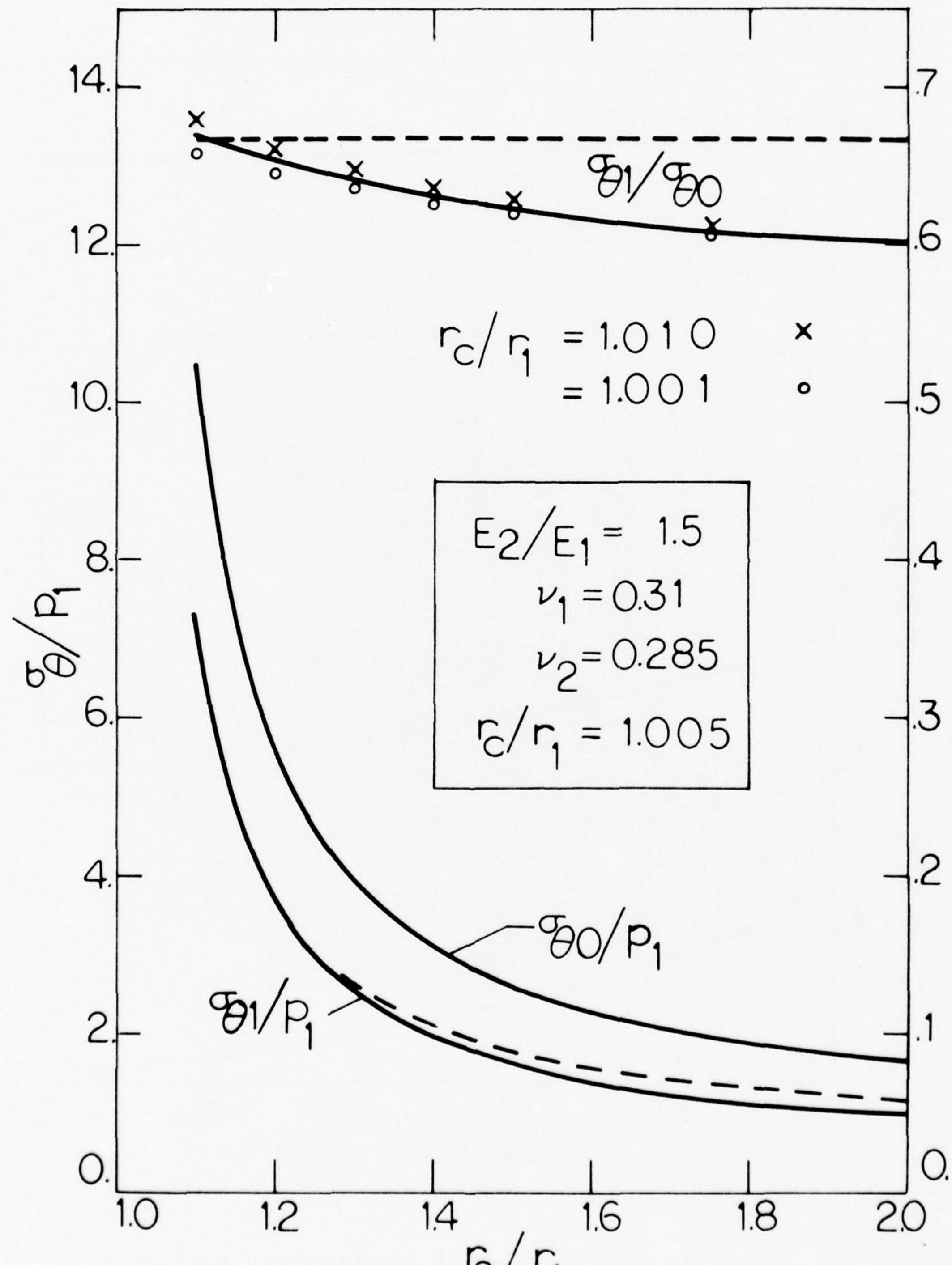

Figure 1. Maximum stress in a plating as a function of wall ratio for Model 1 and Model 2.

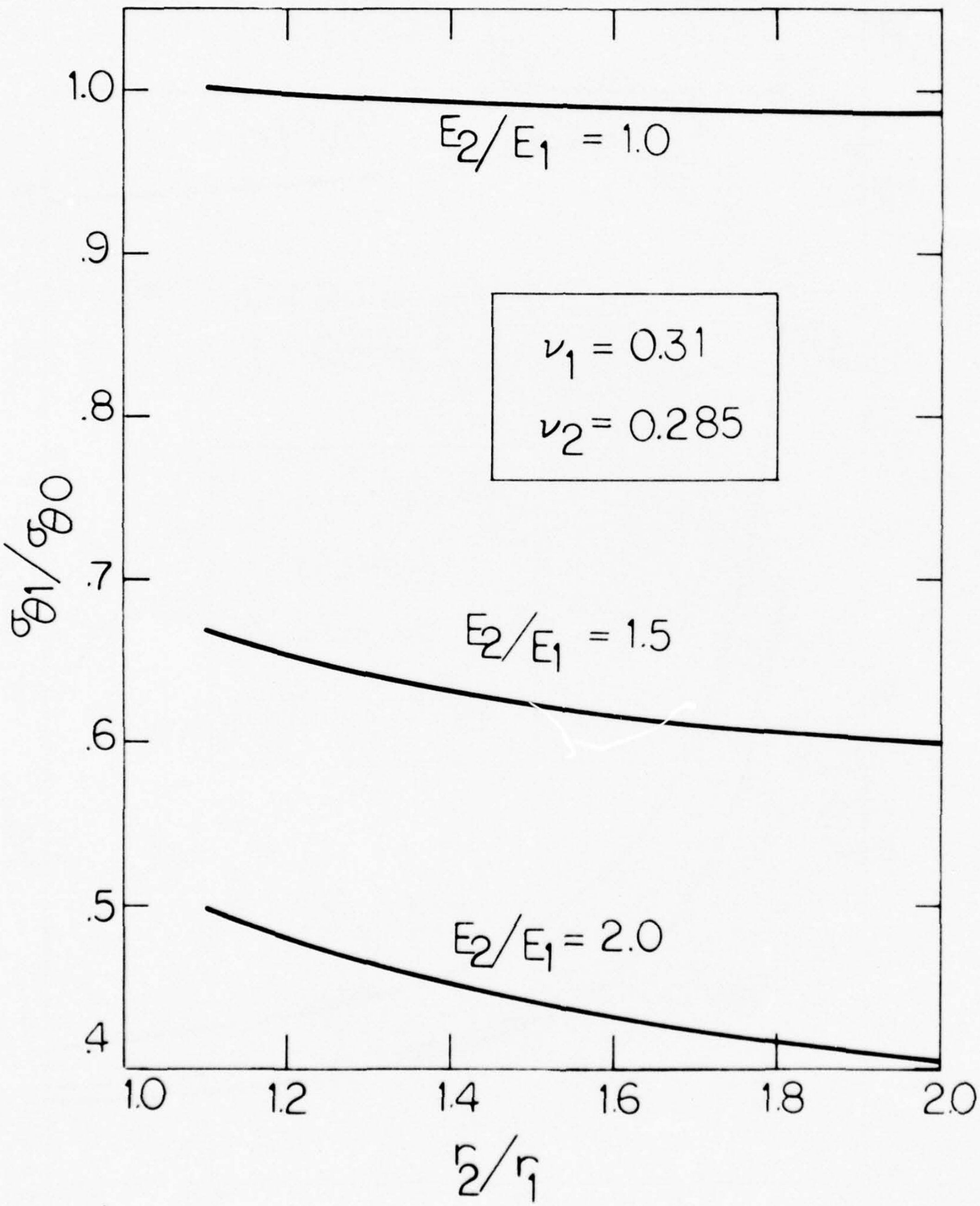

Figure 2. Effect of moduli of elasticity on maximum stress in the plating for Model 2.

Poisson's ratio of the chrome also has a large effect on the stress distribution between the inner and outer tubes. In Fig 3, the graphs of $\sigma_{\theta 1}/\sigma_{\theta o}$ vs r_2/r_1 are given for $\nu_1 = 0$, 0.31 and 0.5 with $\nu_2 = 0.285$ and $E_2/E_1 = 1.5$. The maximum tensile stress is reduced if the plating has a higher value of Poisson's ratio.

For a composite tube subjected to an internal pressure, p_1, when the maximum stress in the inner tube equals the ultimate strength of the chrome, the pressure is denoted by $[p_m]_c$. Similarly, when the maximum stress in the outer tube is equal to the yield point of the steel, the pressure is denoted by $[p_m]_s$. If $[p_m]_c > [p_m]_s$, the steel tube reaches the yield point before the chrome reaches its ultimate strength. The chrome is less likely to crack. If $[p_m]_s/[p_m]_c > 1$, the chrome will crack before we can have the full use of the steel's strength. A plot of $[p_m]_s/[p_m]_c$ vs r_2/r_1 is shown in Fig 4. Curve 1 is based on the average values of E and ν for the chrome. Curve 2 is based on the most favorable mechanical properties for the chrome, while curve 3 is a result based on the most unfavorable values for the chrome. If Mises' yield criterion is used to compute the pressures $[p_m]_s$ and $[p_m]_c$, the ratio $[p_m]_s/[p_m]_c$ is plotted in dotted lines in Fig 4. It shows that $[p_m]_s/[p_m]_c$ is always greater than unity and the chrome will crack before the steel starts to yield.

As mentioned previously, the one-dimensional analysis of the composite tube is a good approximation if the stress components σ_z and τ_{rz} from (21) and (22) are small. Numerically, with $E_2/E_1 = 1.5$, $\nu_1 = 0.31$, $r_c/r_1 = 1.005$, we computed $\tau_{rz}/\sigma_{\theta 1}(r=r_1)$ and $\sigma_{z1}/\sigma_{\theta 1}(r=r_1)$

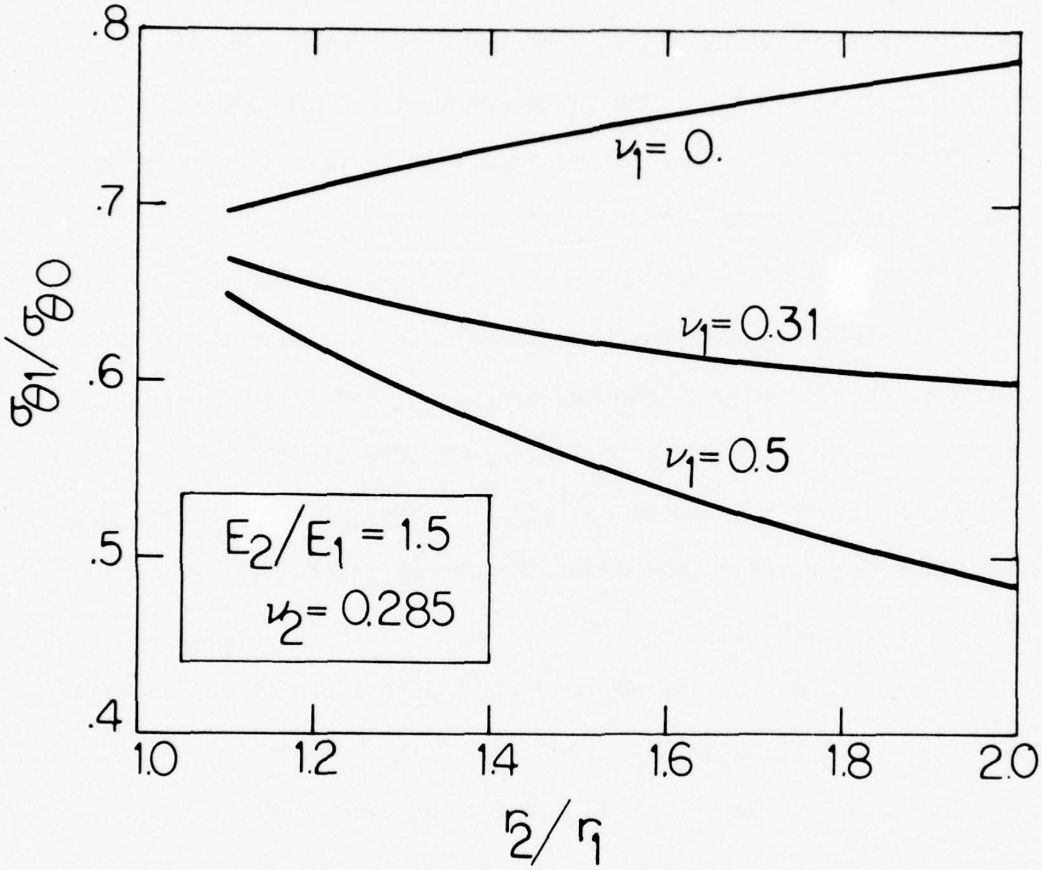

Figure 3. Effect of Poisson's ratio on maximum stress in the plating for Model 2.

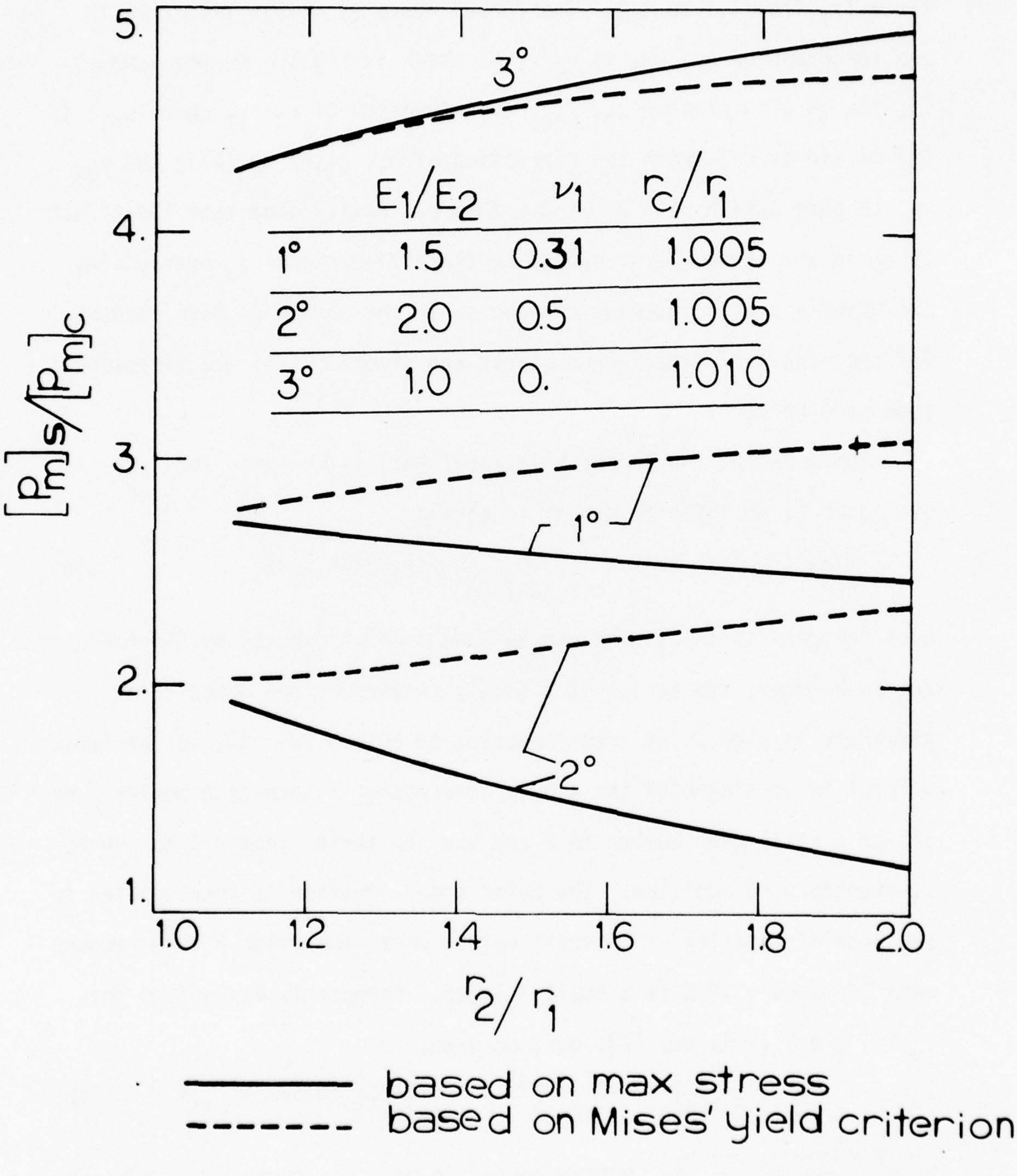

Figure 4. Ratio of failure pressures as a function of wall ratio under various conditions for Model 2.

for r_2/r_1 from 1.1 to 2.0. The former ratio is always less than 1% and the graph of $\sigma_{z1}/\sigma_{\theta 1}$ vs r_2/r_1 is shown in Fig 5. In the same figure, we also plotted $\varepsilon_{\theta 1}'/\varepsilon_{\theta 1}$ as a function of r_2/r_1, where $\varepsilon_{\theta 1}'$ is the strain at $r=r_1$ with the correction of σ_{z1} given by (21), and $\varepsilon_{\theta 1}$ is the same strain with $\sigma_{z1} = 0$. This can easily show that the effect of σ_z in the chrome layer caused by the difference in ε_z between the two materials will increase maximum σ_θ in the chrome no more than 5% for the ranges of material constants and dimensions of the composite tube used here.

For model 3, the improper integral (42), also valid for (43), is evaluated as an infinite sum of integrals

$$\int_0^\infty \sigma_\theta\ (r,k)\sin kzdk = \sum_{n=1}^{\infty} \int_{(n-1)\frac{\pi}{z}}^{\frac{n\pi}{z}} \sigma_\theta(r,k)\sin kzdk \tag{96}$$

Each integral in the series can be numerically computed by Simpson's rule. However, the series is a slowly convergent one whose terms alternate in sign. The transformation of Euler, see [6], is particularly helpful in dealing with the slowly convergent, alternating series. We assign a small even number to N and sum the series from n=1 to n=N by straightforward addition. The Euler transformation is then applied to the remaining series. For small values of z, the value $k = \frac{N\pi}{z}$ becomes very large even if N is a small integer. Asymptotic expansions for $I_\nu(kr)$ and $K_\nu(kr)$, see [7], must be used.

$$I_\nu(z) \simeq \frac{e^z}{\sqrt{2\pi z}} \{1- \frac{\mu-1}{8z} + \frac{(\mu-1)(\mu-9)}{2!(8z)^2} - \frac{(\mu-1)(\mu-9)(\mu-25)}{3!(8z)^3} + \ldots\} \tag{97}$$

---

[6] E. T. Goodwin, et al. MODERN COMPUTING METHODS, Philosophical Library, 2nd Ed., 1961.

[7] M. Abramowitz and I. A. Stegun, editors, HANDBOOK OF MATHEMATICAL FUNCTIONS, National Bureau of Standards, Applied Mathematics Series-55, 1964.

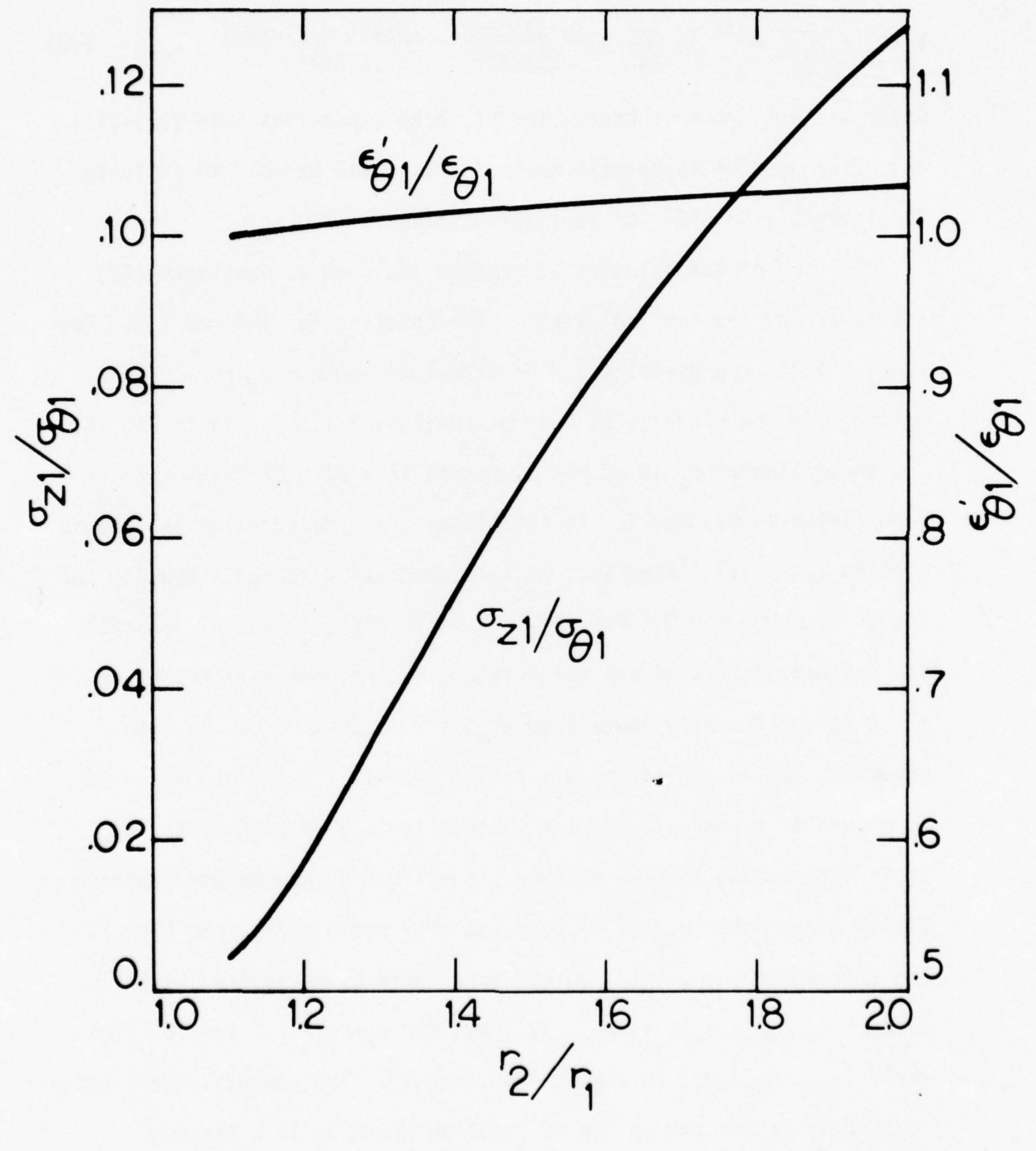

Figure 5. Axial stress σ_z in the plating and its effect are small for various wall ratios

$$K_\nu(z) \approx \sqrt{\frac{\pi}{2z}}\, e^{-z} \{1+ \frac{\mu-1}{8z} + \frac{(\mu-1)(\mu-9)}{2!(8z)^2} + \frac{(\mu-1)(\mu-9)(\mu-25)}{3!(8z)^3} + \ldots\} \quad (98)$$

where $\mu = 4\nu^2$. Upon substitution of these expansions into (37)-(41) and after careful asymptotic analysis, we shall be able to evaluate the integrals in (96) for very large values of k.

The sum of the solution of problem II, such as equations (42) and (43), and the Lame solution is the solution for the model 3. For $r_2/r_1 = 1.25$, the distribution of stress components $\sigma_\theta(r=r_1)$ and $\sigma_z(r=r_1)$ in the vicinity of load discontinuity is plotted in Fig 6. The solid line of σ_z is an odd symmetric in z with the plane stress formulation in problem I. If the plane strain formulation is used in problem I, σ_z is shifted vertically a constant distance, shown in the dotted line for $z \geq 0$. From Fig 6, it is obvious that σ_θ is still the dominant stress in the thick tube. On the bore surface, σ_θ at $z = 0$ is considerably lower than $\sigma_{\theta o}$, the maximum σ_θ of the Lamé solution, and it approaches $\sigma_{\theta o}$ rather rapidly. A maximum value of σ_θ occurs at z near -1, and the maximum is only 3% higher than $\sigma_{\theta o}$. It is interesting to know whether the maximum σ_θ may become substantially higher than $\sigma_{\theta o}$ if we vary the wall ratio r_2/r_1. In Fig 7, the stress component $\sigma_\theta(z)$ on the bore surface, normalized with respect to $\sigma_{\theta o} = \sigma_\theta(z = -\infty)$, is shown for $r_2/r_1 = 1.1$ to 1.5. The ratio $(\sigma_\theta - \sigma_{\theta o})/\sigma_{\theta o}$ is always less than 3%. The change in wall ratio r_2/r_1 only causes the change of location where σ_θ is a maximum.

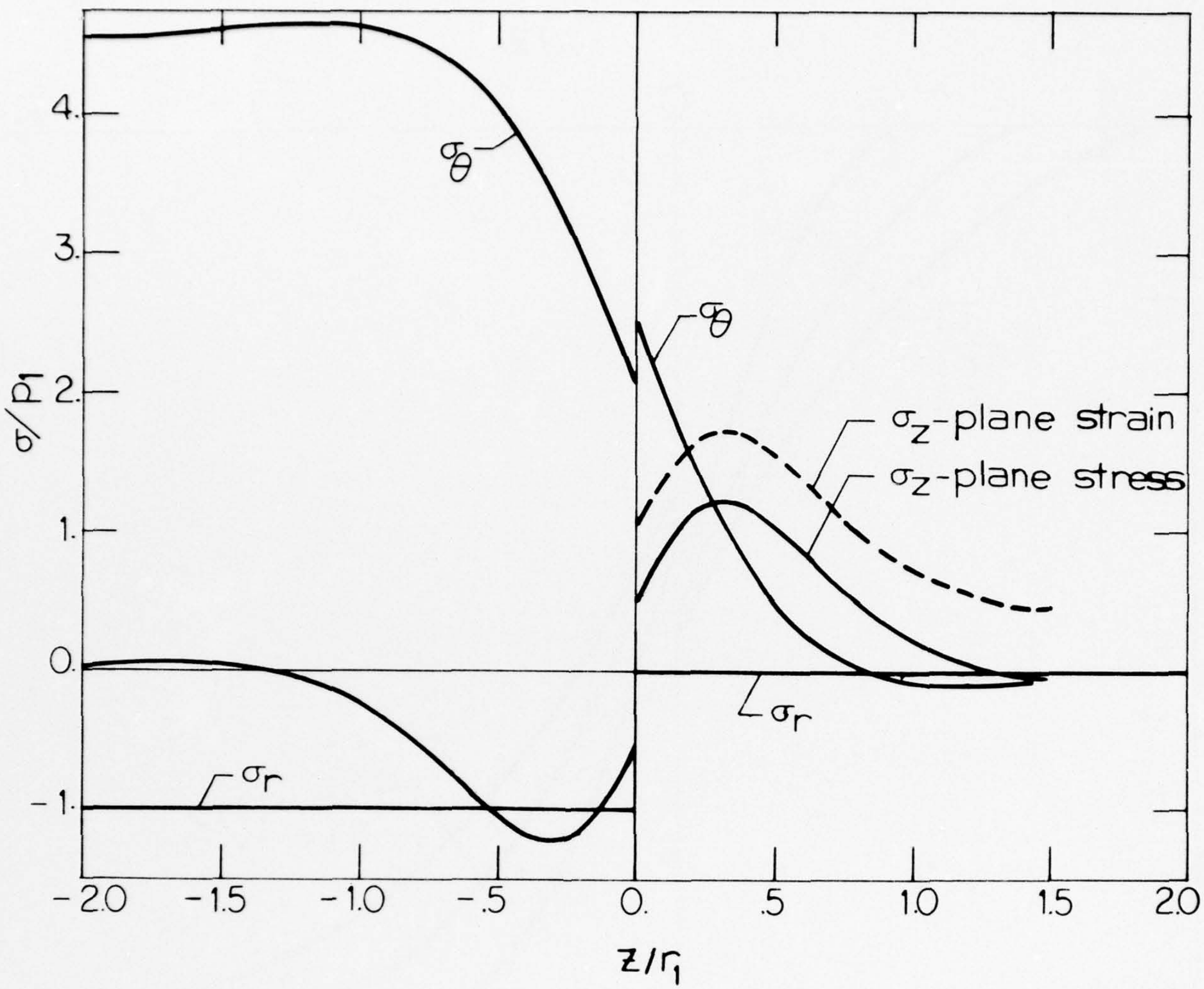

Figure 6. Stresses at r_1 normalized by p_1 in the vicinity of load discontinuity for $r_2/r_1 = 1.25$ for Model 3.

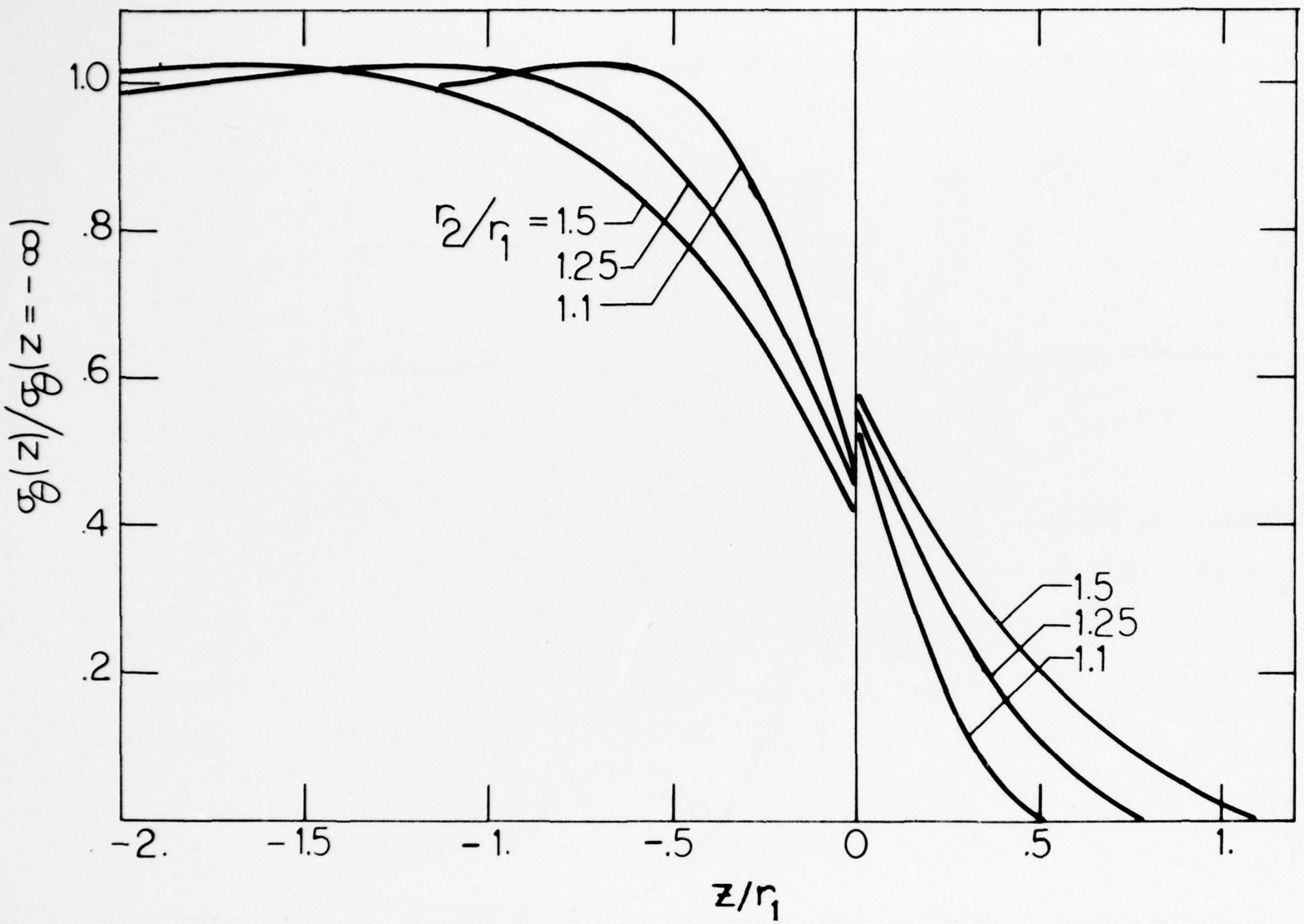

Figure 7. The stress component σ_θ at r_1 normalized by $\sigma_{\theta o}$ in the vicinity of load discontinuity for $r_2/r_1 = 1.1$ to 1.5 for Model 3.

The strain component $E\varepsilon_\theta$ is computed from $E\varepsilon_\theta = \sigma_\theta - \nu(\sigma_r + \sigma_z)$. Let $\varepsilon_{\theta 1}(z)$ of the plating equal $\varepsilon_{\theta 2}(z)$ of the tube at the bore surface, then we may estimate the hoop stress $\sigma_{\theta 1}$ in the chrome as a function of z by $\sigma_{\theta 1}(z) = \frac{E_1}{E_2}[E_2\varepsilon_{\theta 2}(z)]$. Numerical results for $r_2/r_1 = 1.25$, $E_2/E_1 = 1.5$, with the plane stress assumption in problem I, are plotted in Fig 8. Normalized by the corresponding $\sigma_{\theta o}$, the numerical results of $E_2\sigma_{\theta 2}(z)/\sigma_{\theta o}$ for other values of r_2/r_1 are shown in Fig 9. The tensile stress in the thin plating can be estimated for any value of E_2/E_1 from Fig 9.

For model 4, work is being carried out on numerical analysis, but is not complete at this time. The method of computation for model 3 can be followed closely here. The asymptotic analysis for both extreme cases $k \to 0$ and $k \to \infty$ must be carefully worked out for (56), (57), (58) and then for (55) in order to evaluate the integrals (60) and (61). This is quite time consuming. The interesting points in the numerical results of model 4 are to see (1) whether σ_z in the chrome layer, due to the load discontinuity, is still relatively unimportant as in model 3 and (2) whether the maximum σ_z in the chrome layer remains only slightly higher than that obtained in model 2.

To compute thermal stresses in a composite tube, $\alpha_2 = 6.5 \times 10^{-6}$ in./in./°F is used for the steel, and the following basic values are used for other parameters: $r_2/r_1 = 1.5$, $r_c/r_1 = 1.005$, $K_2/K_1 = 0.5$, $\alpha_1 = 3.5 \times 10^{-6}$ in./in./°F, $T_1 = 800°F$ and $T_1 - T_2 = \Delta T = 400°F$, the temperatures suggested by Joseph Throop based on his study of thermal

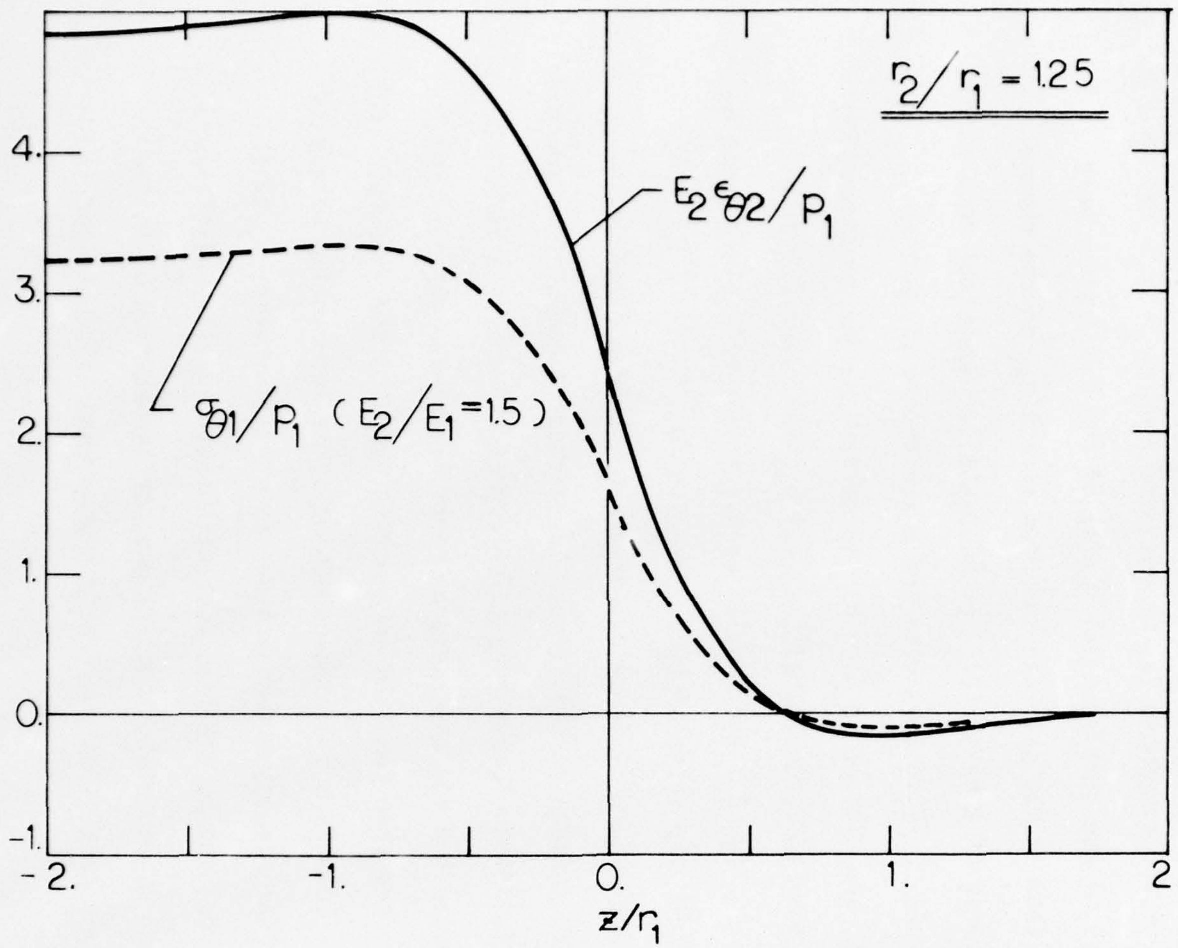

Figure 8. Estimated $\sigma_{\theta 1}$ in the plating at r_1 normalized by p_1 as a function of z/r_1 for $r_2/r_1 = 1.25$, $E_2/E_1 = 1.5$ for Model 3.

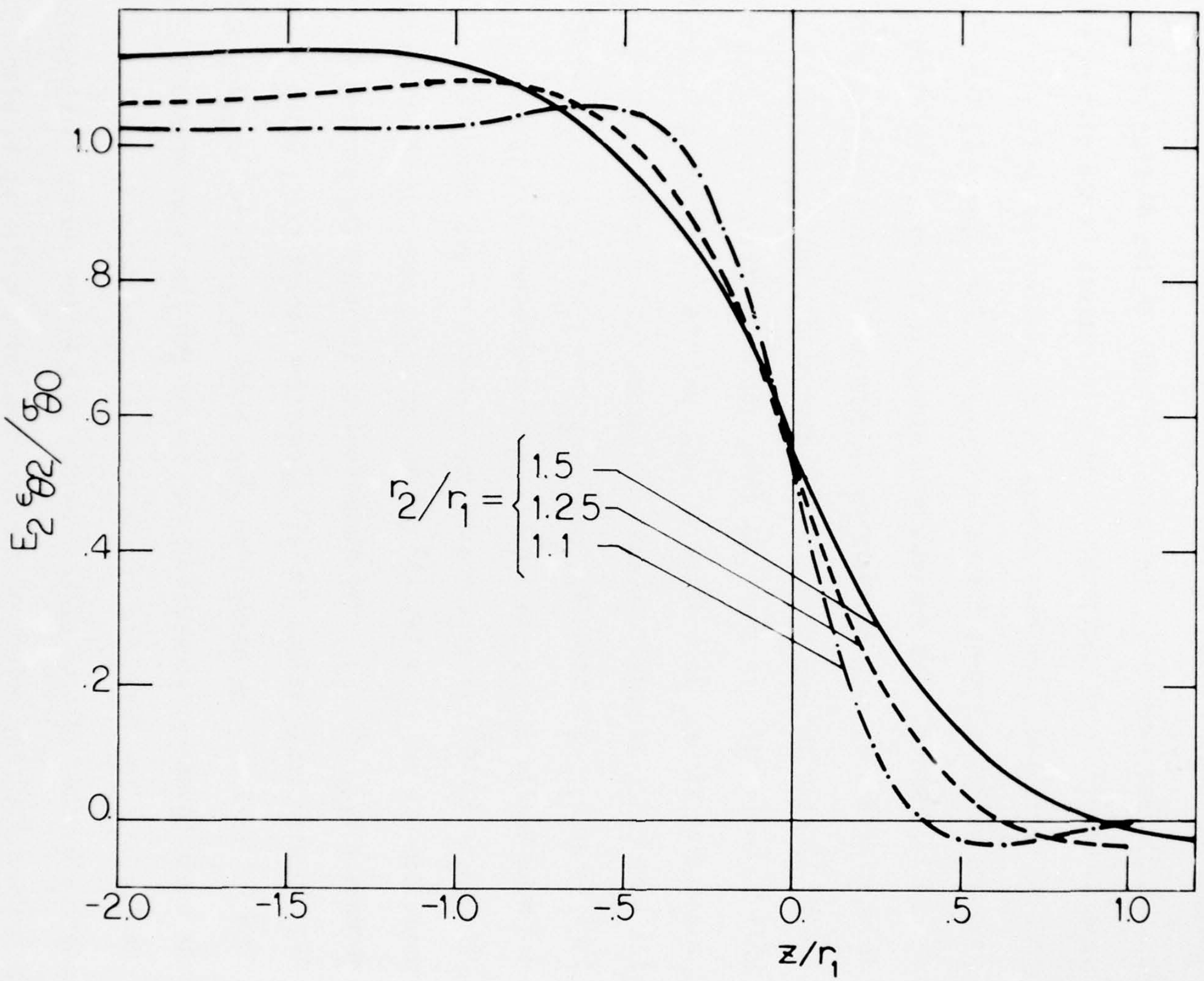

Figure 9. $E_2\varepsilon_{\theta 2}$ at r_1 normalized by $\sigma_{\theta o}$ as a function of z/r_1 for r_2/r_1 = 1.1 to 1.5 for Model 3.

effects on autofrettaged residual stresses in rapid fire gun barrels, an unpublished research. The radial stresses in the plating and the tube are found to be negligible. The axial stress in the plating may also be neglected. The hoop stress in the plating may be tensile or compressive depending on the ratio of α_2/α_1. For $\alpha_2/\alpha_1 > 1$, the stress is tensile. The maximum hoop stress is at $r=r_c$. The difference in hoop stress at $r=r_c$ and at $r=r_1$ is very small since the thickness of the plating is very thin. In our discussion, only $\sigma_\theta(r=r_1) = \sigma_{\theta 1}$ will be mentioned. In the thick tube, the hoop stress varies from compressive at $r=r_c$ to tensile at $r=r_2$, and the axial stress is about the same order of magnitude and also varies from compressive at r_c to tensile at r_2. The stresses, $\sigma_{\theta 2c} = \sigma_{\theta 2}(r=r_c)$ and $\sigma_{z2c} = \sigma_{z2}(r=r_c)$, are numerically largest in the ranges of parameters of interest. Using $\sigma_u = 40\text{x}10^3$ psi as the ultimate strength of the chrome to normalize $\sigma_{\theta 1}$ and $\sigma_y = 165\text{x}10^3$ psi as the yield point of the steel to normalize $\sigma_{\theta 2c}$ and σ_{z2c}, the dimensionless stresses are plotted in Fig 10 with basic values for all parameters except r_2/r_1 which varies from 1.1 to 2.0. The heavy line gives both $-\sigma_{\theta 2c}/\sigma_y$ and $-\sigma_{z2c}/\sigma_y$ with the upper boundary representing the former and the lower boundary the latter. The influence of the thermal conductivity is small. Increasing the ratio of K_2/K_1 from 0.5 to 2.0, the change in stresses is within 2%. The effect of the thickness of the plating is also small. The stress variation is found to be no more than 1% if the thickness is doubled from $(r_c-r_1)/r_1 = 0.005$ to 0.01.

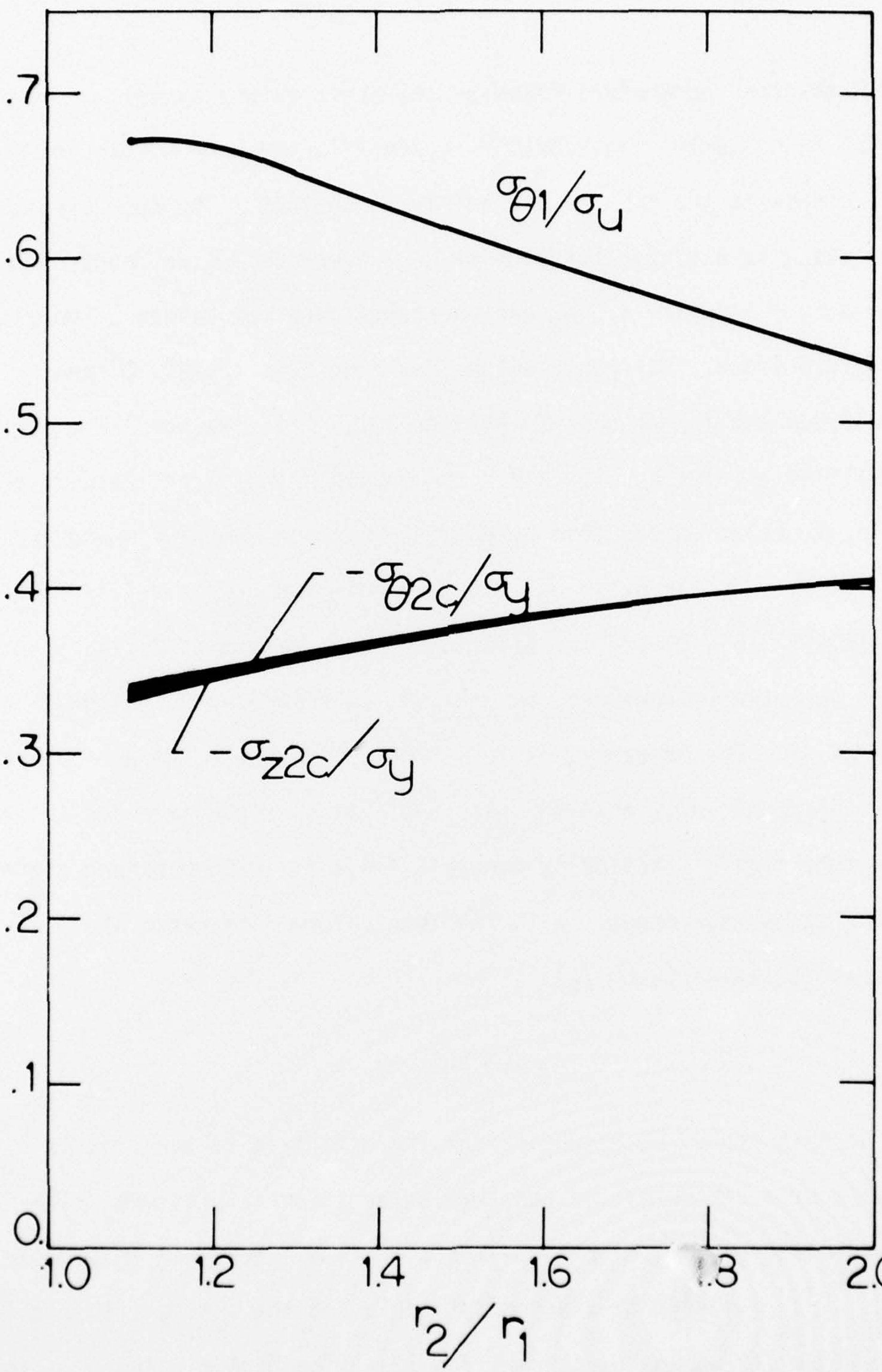

Figure 10. Dimensionless stresses in the steel tube and the plating as a function of wall ratio due to steady state temperature gradient.

With other parameters fixed at the basic values except α_1 varying from $3.5x10^{-6}$ to $9.5x10^{-6}$ in./in./°F, the hoop stress and the axial stress in the tube remain nearly a constant. The hoop stress in the plating is a linear function of α_1. Numerically, we found $\sigma_{\theta 1} = A_1\alpha_1 + A_2$ where A_1, A_2 are constants once the values of parameters are fixed. For basic values, we have $A_1 = -23120x10^6$ and $A_2 = 105500$ and the results in psi for $\sigma_{\theta 1}$. The stresses are $\sigma_{\theta 1} = 24572$ and -114140 psi for $\alpha_1 = 3.5x10^{-6}$ and $9.5x10^{-6}$ in./in./°F respectively. The linear relation can also be obtained between the stress and the temperature. We can write $\sigma_{\theta 1} = B_1T_1 + B_2T_2$ and $\sigma_{\theta 2c} = D_1T_1 + D_2T_2$ where B_1, B_2, D_1, D_2 are functions of other parameters. Using basic values for other parameters, $B_1 =-21.68$, $B_2 = 104.79$, $D_1 = -153.15$ and $D_2 = 152.07$. For instance, if $T_1 = 800°F$, $T_2 = 400°F$, we have $\sigma_{\theta 1} = 24572$ psi, $\sigma_{\theta 2c} = -61692$ psi. We note that the stresses in the thick tube remain practically constant for a fixed temperature difference but the stress $\sigma_{\theta 1}$ changes with the temperature difference and the temperature level (T_1 or T_2).

CONCLUSIONS

In this report we have confined our attention to the elastic analysis of a chrome-plated gun tube under internal pressure. The Lamé solution gives a close estimate of maximum stress in the chrome layer. The reduction of elasticity modulus of the chrome will reduce the maximum stress in the chrome (Fig 2). The higher value of Poisson's ratio for the chrome will also reduce the maximum stress in the chrome

(Fig 3). The increase in thickness of the chrome layer will cause a slight increase in maximum stress in the chrome. However, the increase in stress is so small that the thickness of the chrome should be considered from other factors. The stress distributions in both chrome and steel tubes are very sensitive to the wall ratio r_2/r_1. Except in extreme cases where the Poisson's ratio of the chrome is small, the maximum stress in the chrome, $\sigma_\theta(r=r_1)$, increases faster than that in the steel ($\sigma_\theta(r=r_c)$) as we decrease the wall ratio. This means that for a tube with a smaller wall ratio, the stress in the chrome is larger when the maximum stress in the steel reaches the same level.

It seems that the load discontinuity only increases the maximum stress slightly. However, further numerical results must be obtained for model 4 to confirm this conclusion.

From the stress analysis based on the linear theory of elasticity, the chrome layer is likely to crack when the steel tube is subjected to an internal pressure which produces a maximum stress close to the yield point of the gun steel.

For a steady state temperature field with the highest temperature T_1 at r_1, the thick tube has stresses σ_θ and σ_z compressive at r_c and tensile at r_2 which, similar to the residual stress in an autofrettaged tube, will strengthen the tube to sustain a higher internal pressure. The thermal stress alone in the temperature range of interest, will probably not cause a crack in the chrome layer. For $\alpha_1 = 3.5\times10^{-6}$ in./in./°F, the hoop stress $\sigma_{\theta 1}$ in the chrome is tensile, which will add to

the high tensile stress due to the internal pressure. The combination of the internal pressure and the temperature field will produce a much too high tensile stress in the chrome to cause cracks. However, if we can choose a plating material with a high linear thermal expansion coefficient, say $\alpha_1 \geq 6.5 \times 10^{-6}$ in./in./°F, then a compressive thermal stress shall be introduced in the plating which might be helpful in eliminating part of the tensile stress σ_θ due to the internal pressure.

REFERENCES

1. S. Timoshenko and J. N. Goodier, THEORY OF ELASTICITY, McGraw-Hill Book Co., New York, 1951.
2. C. J. Tranter, "On the Elastic Distortion of a Cylindrical Hole by a Localized Hydrostatic Pressure", Quarterly of Applied Mathematics, No. 4, p. 298, 1946.
3. O. L. Bowie, "Elastic Stresses Due to a Semi-Infinite Band of Hydrostatic Pressure Acting Over a Cylindrical Hole in an Infinite Solid", Quarterly of Applied Mathematics, No. 5, p. 100, 1947.
4. A. W. Rankon, "Shrink-Fit Stresses and Deformations", Journal of Applied Mechanics, Vol. 11, p. A77, 1944.
5. P. P. Radkowski, J. Bluhm, O. L. Bowie, "Stresses and Strains in Elastic, Thick-Walled, Circular Cylinders Resulting From Axially Symmetric Loadings", Technical Report WAL No. 893/172, Dec. 1954.
6. E. T. Goodwin, et al. MODERN COMPUTING METHODS, Philosophical Library, 2nd Ed., 1961.
7. M. Abramowitz and I. A. Stegun, editors, HANDBOOK OF MATHEMATICAL FUNCTIONS, National Bureau of Standards, Applied Mathematics Series-55, 1964.

WATERVLIET ARSENAL INTERNAL DISTRIBUTION LIST

May 1976

	No. of Copies
COMMANDER	1
DIRECTOR, BENET WEAPONS LABORATORY	1
DIRECTOR, DEVELOPMENT ENGINEERING DIRECTORATE	1
ATTN: RD-AT	1
RD-MR	1
RD-PE	1
RD-RM	1
RD-SE	1
RD-SP	1
DIRECTOR, ENGINEERING SUPPORT DIRECTORATE	1
DIRECTOR, RESEARCH DIRECTORATE	2
ATTN: RR-AM	1
RR-C	1
RR-ME	1
RR-PS	1
TECHNICAL LIBRARY	5
TECHNICAL PUBLICATIONS & EDITING BRANCH	2
DIRECTOR, OPERATIONS DIRECTORATE	1
DIRECTOR, PROCUREMENT DIRECTORATE	1
DIRECTOR, PRODUCT ASSURANCE DIRECTORATE	1
PATENT ADVISORS	1

EXTERNAL DISTRIBUTION LIST

December 1976

1 copy to each

OFC OF THE DIR. OF DEFENSE R&E
ATTN: ASST DIRECTOR MATERIALS
THE PENTAGON
WASHINGTON, D.C. 20315

CDR
US ARMY TANK-AUTMV COMD
ATTN: AMDTA-UL
AMSTA-RKM MAT LAB
WARREN, MICHIGAN 48090

CDR
PICATINNY ARSENAL
ATTN: SARPA-TS-S
SARPA-VP3 (PLASTICS TECH EVAL CEN)
DOVER, NJ 07801

CDR
FRANKFORD ARSENAL
ATTN: SARFA
PHILADELPHIA, PA 19137

DIRECTOR
US ARMY BALLISTIC RSCH LABS
ATTN: AMXBR-LB
ABERDEEN PROVING GROUND
MARYLAND 21005

CDR
US ARMY RSCH OFC (DURHAM)
BOX CM, DUKE STATION
ATTN: RDRD-IPL
DURHAM, NC 27706

CDR
WEST POINT MIL ACADEMY
ATTN: CHMN, MECH ENGR DEPT
WEST POINT, NY 10996

CDR
HQ, US ARMY AVN SCH
ATTN: OFC OF THE LIBRARIAN
FT RUCKER, ALABAMA 36362

CDR
US ARMY ARMT COMD
ATTN: AMSAR-PPW-IR
AMSAR-RD
AMSAR-RDG
ROCK ISLAND, IL 61201

CDR
US ARMY ARMT COMD
FLD SVC DIV
ARMCOM ARMT SYS OFC
ATTN: AMSAR-ASF
ROCK ISLAND, IL 61201

CDR
US ARMY ELCT COMD
FT MONMOUTH, NJ 07703

CDR
REDSTONE ARSENAL
ATTN: AMSMI-RRS
AMSMI-RSM
ALABAMA 35809

CDR
ROCK ISLAND ARSENAL
ATTN: SARRI-RDD
ROCK ISLAND, IL 61202

CDR
US ARMY FGN SCIENCE & TECH CEN
ATTN: AMXST-SD
220 7TH STREET N.E.
CHARLOTTESVILLE, VA 22901

DIRECTOR
US ARMY PDN EQ. AGENCY
ATTN: AMXPE-MT
ROCK ISLAND, IL 61201

EXTERNAL DISTRIBUTION LIST (Cont)

1 copy to each

CDR
US NAVAL WPNS LAB
CHIEF, MAT SCIENCE DIV
ATTN: MR. D. MALYEVAC
DAHLGREN, VA 22448

DIRECTOR
NAVAL RSCH LAB
ATTN: DIR. MECH DIV
WASHINGTON, D.C. 20375

DIRECTOR
NAVAL RSCH LAB
CODE 26-27 (DOCU LIB.)
WASHINGTON, D.C. 20375

NASA SCIENTIFIC & TECH INFO FAC
PO BOX 8757, ATTN: ACQ BR
BALTIMORE/WASHINGTON INTL AIRPORT
MARYLAND 21240

DEFENSE METALS INFO CEN
BATTELLE INSTITUTE
505 KING AVE
COLUMBUS, OHIO 43201

MANUEL E. PRADO / G. STISSER
LAWRENCE LIVERMORE LAB
PO BOX 808
LIVERMORE, CA 94550

DR. ROBERT QUATTRONE
CHIEF, MAT BR
US ARMY R&S GROUP, EUR
BOX 65, FPO N.Y. 09510

2 copies to each

CDR
US ARMY MOB EQUIP RSCH & DEV COMD
ATTN: TECH DOCU CEN
FT BELVOIR, VA 22060

CDR
US ARMY MAT RSCH AGCY
ATTN: AMXMR - TECH INFO CEN
WATERTOWN, MASS 02172

CDR
WRIGHT-PATTERSON AFB
ATTN: AFML/MXA
OHIO 45433

CDR
REDSTONE ARSENAL
ATTN: DOCU & TECH INFO BR
ALABAMA 35809

12 copies

CDR
DEFENSE DOCU CEN
ATTN: DDC-TCA
CAMERON STATION
ALEXANDRIA, VA 223.4

NOTE: PLEASE NOTIFY CDR, WATERVLIET ARSENAL, ATTN: SARWV-RT-TP, WATERVLIET, N.Y. 12189, IF ANY CHANGE IS REQUIRED TO THE ABOVE.